Biochimica et Biophysica Acta 1814 (2011) 1001–1020

Contents lists available at ScienceDirect

Biochimica et Biophysica Acta

journal homepage: www.elsevier.com/locate/bbapap

Review

Dynamics of protein folding: Probing the kinetic network of folding–unfolding transitions with experiment and theory ☆

Ginka S. Buchner [a,b], Ronan D. Murphy [c], Nicolae-Viorel Buchete [c,d,*], Jan Kubelka [a,*]

[a] Department of Chemistry, University of Wyoming, Laramie, WY 82071, USA
[b] Universität Würzbug, Würzburg, Germany
[c] School of Physics, University College Dublin, Belfield, Dublin 4, Ireland
[d] Department of Chemistry, Boston University, Boston, MA 02215, USA

ARTICLE INFO

Article history:
Received 30 June 2010
Received in revised form 14 September 2010
Accepted 16 September 2010
Available online 29 September 2010

Keywords:
Protein folding
Experimental kinetics
Dynamics
Elementary events in folding
Ultra-fast folding
Downhill folding
Protein folding speed limit
Free-energy surface
Molecular dynamics simulations
Master equations
Coarse graining

ABSTRACT

The problem of spontaneous folding of amino acid chains into highly organized, biologically functional three-dimensional protein structures continues to challenge the modern science. Understanding how proteins fold requires characterization of the underlying energy landscapes as well as the dynamics of the polypeptide chains in all stages of the folding process. In recent years, important advances toward these goals have been achieved owing to the rapidly growing interdisciplinary interest and significant progress in both experimental techniques and theoretical methods. Improvements in the experimental time resolution led to determination of the timescales of the important elementary events in folding, such as formation of secondary structure and tertiary contacts. Sensitive single molecule methods made possible probing the distributions of the unfolded and folded states and following the folding reaction of individual protein molecules. Discovery of proteins that fold in microseconds opened the possibility of atomic-level theoretical simulations of folding and their direct comparisons with experimental data, as well as of direct experimental observation of the barrier-less folding transition. The ultra-fast folding also brought new questions, concerning the intrinsic limits of the folding rates and experimental signatures of barrier-less "downhill" folding. These problems will require novel approaches for even more detailed experimental investigations of the folding dynamics as well as for the analysis of the folding kinetic data. For theoretical simulations of folding, a main challenge is how to extract the relevant information from overwhelmingly detailed atomistic trajectories. New theoretical methods have been devised to allow a systematic approach towards a quantitative analysis of the kinetic network of folding–unfolding transitions between various configuration states of a protein, revealing the transition states and the associated folding pathways at multiple levels, from atomistic to coarse-grained representations. This article is part of a Special Issue entitled: Protein Dynamics: Experimental and Computational Approaches.

© 2010 Elsevier B.V. All rights reserved.

1. Introduction

The problem of spontaneous folding of protein amino acid chains into compact, highly organized three-dimensional structures continues to challenge the modern science [1]. The protein folding research has two primary objectives. The first is to be able to predict the three-dimensional protein structure from its amino acid sequence. Protein amino acid sequences are encoded in genes, but protein structures are key to understanding the mechanisms that control their ultimate biological functionality. Protein folding is therefore the final step in translation of the genetic information to biological function. As the wealth of amino acid sequence information obtained by rapid new gene sequencing methods continues to severely outpace the experimental determination of protein structures, the significance of reliable structure prediction methods is enormous.

The second main goal is to understand the mechanism of protein three-dimensional structure formation. The protein folding mechanism may not seem as directly biologically relevant, as folding occurs spontaneously and the biological function is tied predominantly to the folded structure. However, in many cases protein folding or unfolding is an integral part of the biochemical function and of other biocellular processes, such as translocation and degradation. Defects in folding can lead to severe disorders, illness and death [2]. While the folding mechanism of a protein with known structure may appear as an easier problem to tackle than predicting unknown structures, it is no less daunting task. Determination of the folding mechanism means piecing together the microscopic, atomic-level pathways along which proteins pick their way through all the possible conformations in the search for their folded states. Although the folded structure is known, it represents

☆ This article is part of a Special Issue entitled: Protein Dynamics: Experimental and Computational Approaches.

* Corresponding authors. Buchete is to be contacted at School of Physics, University College Dublin, Belfield, Dublin 4, Ireland. Kubelka, Department of Chemistry, University of Wyoming, Laramie, WY 82071, USA.
E-mail addresses: buchete@ucd.ie (N.-V. Buchete), jkubelka@uwyo.edu (J. Kubelka).

1570-9639/$ – see front matter © 2010 Elsevier B.V. All rights reserved.
doi:10.1016/j.bbapap.2010.09.013

only a single point in the vast space of unknowns. Ultimately, understanding how proteins fold would also provide the solution to the first problem: if the physical mechanism of folding could be simulated, the unknown three-dimensional structures could be predicted. That most successful protein structure prediction methods completely bypass the folding process, relying on the databases of known structures [3], is another testimony to the difficulty of pursuing physics-based mechanistic studies of folding [4,5].

The intriguing efficiency and robustness of protein folding along with the great practical significance of uncovering its principles have stimulated a massive interdisciplinary research effort. While the general solution still appears far beyond the horizon, tremendous progress has been made. Especially during the last two decades a series of important advances in both theory and experiment opened new avenues and opportunities for understanding the principles behind protein folding. Introduction of high time resolution experimental methods in the late 1990s made possible determination of the timescales of elementary events in folding, such as polypeptide chain collapse and formation of local secondary structure [6,7]. The fast time-resolved experiments led to the discovery of proteins that fold on submillisecond and microsecond timescales, indicating that the free-energy barriers to folding are marginally high and, possibly, can disappear altogether. The barrier-less or "downhill" folding in principle allows experimental detection of the intermediates along the folding pathways [8], which in slower folding proteins are not observable due to their high free energy. Particularly in combination with the rapidly advancing single molecule detection techniques [9,10] the "downhill" folding proteins promise probing the microscopic folding pathways one molecule at a time.

Another important significance of ultra-fast folding proteins is that it is becoming possible to simulate their folding at atomic level owing to the increasing power of the modern computers and new massively parallel algorithms [11,12]. The all-atom folding simulations, if accurate, can provide the most detailed picture of the folding mechanism. The ultra-fast folding proteins offer an opportunity for direct comparison between the atomic level folding simulations and experiments.

These exciting properties stimulated a considerable interest and search for even faster folding proteins with the ultimate goal to eliminate the folding free-energy barriers. The studies of ultra-fast folding also inspired new kinds of questions, concerning the analysis of the kinetic data as the simple chemical mass action laws are no longer justified for low or absent free-energy barriers. Additional questions arose about the experimental signatures and identification of barrier-less folding, in particular the significance of "strange" non-exponential or probe-dependent kinetics [13,14]. The related problem is how fast proteins can fold without the free-energy barrier: the protein folding "speed limit" [15,16]. These new questions underline the importance of understanding the dynamics of the polypeptide chains, timescales of the elementary folding steps and factors that affect the protein motions during folding.

In this review, we attempt to summarize the current knowledge and understanding of the protein folding dynamics and highlight some of the recent advances from both experimental and theoretical perspectives. After briefly outlining the basic concepts of kinetics and dynamics in protein folding, we first focus on the experimental studies, starting with a general overview of the experimental methods and approaches. Special emphasis is devoted to high time resolution experiments, which have been instrumental in uncovering the hierarchy of the timescales of the elementary processes in protein folding, as well as in the discovery and investigations of the ultra-fast folding proteins. Next we review the applications of these methods to the elementary folding events in model peptides, dynamics of denatured protein chains and ultra-fast protein folding. We discuss the issues that arose with the ultra-fast and downhill folding, namely the interpretation of the experimental data, non-exponential and probe-dependent kinetics, and the protein folding "speed limit". Finally, we address the effects of solvent viscosity and internal friction on the folding rates.

The final part of this review discusses the theoretical modeling of the protein folding kinetics, focusing in particular on kinetic network descriptions of folding–unfolding processes. While this approach is only one aspect of the significant recent developments in the computational and theoretical studies of protein folding dynamics, we find it to be an exciting and promising framework for making direct connections with experiments. Nevertheless, we acknowledge significant advances being made in related topics such as understanding the effect of molecular crowding [17,18] and the specific folding–unfolding dynamics of intrinsically unstructured proteins [19–21], to mention just a few.

Computational kinetic network models are typically based on the idea that simulations have the promise to offer an exhaustively detailed description of both the thermodynamics and the detailed kinetics of folding proteins as they navigate the free-energy landscapes along various folding–unfolding routes. The complexity of these systems leads to well-known problems arising from the limited accuracy of the molecular interaction potentials being used [4,22–24] and from the limited sampling allowed by current computational hardware and software [12]. A third, much less acknowledged limitation, yet as important as the former two, is the need for a theoretical framework that could be used to describe in a systematic, quantitative manner the possible folding mechanisms of a large class of proteins, under various environmental conditions [25]. We will present several recent advances in the protein folding simulation and analysis methods that try to address these problems.

2. Dynamics and kinetics in protein folding

Since protein folding is evolution of the folded structure in time, dynamics is an essential part of the folding process. In general, folding can be viewed as the motion of the polypeptide chain on a complex energy landscape [26,27]. The complexity arises on one hand from the vast number of degrees of freedom available to the polypeptide chain, and on the other from the intricate network of weak, non-covalent interactions, which stabilize the native and intermediate structures. The folding pathways are controlled by two main factors: first the thermodynamic stability of the partially folded intermediates, and second the dynamics of the polypeptide chain motions through which these structures are sampled. Both the thermodynamic and dynamic components contribute to the kinetics of folding. Kinetics in general refers to the macroscopic change in the population of protein conformational states in time. Since the evolution of the folded or unfolded population with time can be experimentally observed, measurements of folding kinetics are the primary experimental tool for characterizing the folding process.

2.1. Folding kinetics and rate theories

Despite the vast number of degrees of freedom involved, the experimental kinetics of protein folding is often indicative of a very simple process, which can be described by a kinetic scheme containing only two, or a small number of macroscopic states [28]. Such simple kinetics arises from separation in timescales between the re-equilibration of many possible unfolded or partially folded configurations and the main folding transition [29–31]. Folding is much slower because the folded state can be directly reached, by an elementary conformational step, from only a small fraction of the chain configurations. These "gateway" states constitute a bottleneck on the folding pathways, which can be represented as a free-energy barrier to folding, provided that a suitable reaction coordinate or coordinates to measure the degree of folding can be defined. Although it is not completely clear what the suitable coordinates are and even whether a single or a few such parameters exist, the energy landscape theory asserts that without much loss of kinetic information protein folding can be captured by one or a small number of reaction coordinates [32,33]. While such reaction coordinates are seldom accessible experimentally [34,35], their

existence allows systematic conceptual treatments of folding kinetics based on reaction rate theories.

For the simple, two-state like process, the macroscopic folding rate constant can be written as:

$$k_F = k_0 \exp\left(-\Delta G^{\ddagger} / k_B T\right) \quad (1)$$

where $\Delta G^{\ddagger}$ is the free-energy barrier height, k_B is Boltzmann constant and T is the absolute temperature. The dynamics of motions of the polypeptide chain along the reaction coordinate is contained in the pre-exponential factor k_0. If the value of k_0 were known, the measurement of the macroscopic folding rates would allow straightforward calculations of the free-energy barriers to folding. For this reason, the frequency factor of the transition state theory is often invoked:

$$k_0 = k_B T/h \quad (2)$$

where h is Planck constant. While this expression is appealing due to its simplicity, it was derived for gas phase, small molecule reactions and is not generally valid for reactions in solution. The value of $k_BT/h = 6\times10^{12}\ s^{-1}$ at 300 K is likely several orders of magnitude too high for large-scale motions of the polypeptide chains, which furthermore collide with the solvent molecules as well as with themselves. The chain dynamics should correspond to the high friction limit, which is described by Kramers' theory of diffusive escape over a free-energy barrier [36,37]:

$$k_0 = \frac{\omega_0 \omega_B D_B}{2\pi k_B T} = \frac{\omega_0 \omega_B}{2\pi\xi} \quad (3)$$

where ω_0 and ω_B are (angular) frequencies that characterize the curvature of the free-energy profile at the unfolded well and (inverted) barrier top, respectively, D_B is the diffusion constant at the barrier top, ξ is the coefficient of friction and the last equality follows from Einstein relation: $D_B = k_BT/\xi$. The friction is proportional to the macroscopic viscosity η of the surrounding medium, which, neglecting the contribution of the "internal" friction (see below, Section 3.3.4), is the solvent. According to the Kramers' expression (Eq. (3)), the rate is therefore inversely proportional to the solvent viscosity, which can be tested experimentally [38]. However, in practice, Kramers' escape rate does not provide the means for independent, quantitative estimation of the folding rate prefactors as the frequency terms as well as the diffusion (friction) constant are unknown.

2.2. Dynamics on folding free-energy surfaces

Both transition state and Kramers' reaction rate theories are based on the fundamental assumption of a high free-energy barrier ($\Delta G^{\ddagger} \gg k_BT$). High free-energy barriers simplify the analysis of the folding kinetics and effects of perturbations, such as mutations [39], on the folding rates. Unfortunately, high barriers also prevent direct observation of the partially folded states and their inter-conversions during folding due to their undetectably low populations. For the theoretical simulations, low probability of crossing high free-energy barriers means sampling the huge conformational space of the polypeptide chains for intractably long simulation times. These limitations are eliminated if the folding free-energy barriers become small (a few k_BT or less) [40]. For small barriers the timescales of the conformational dynamics become comparable to those of the overall folding. This opens the possibility for direct measurements of the protein dynamics from the macroscopic folding kinetics [41]. Furthermore, for the small and ultra-fast folding proteins all-atom molecular dynamics (MD) simulations of folding have become possible [11,12]. Unlike the kinetic experiments, which are inherently limited by the detectable structural detail, the simulations, if accurate, can provide the most detailed, atomic level picture of folding. An important new role of the ultra-fast folding proteins therefore is as experimental benchmarks for the theoretical folding simulations [42–44].

The absence of the activation term in the rate expression (Eq. (1)) suggests that the folding dynamics can be directly measured. However, for small barriers, the assumptions of the rate theories presented above are also no longer valid. In fact, in the limit of no free-energy barrier, there is no clear boundary between the folded and unfolded states. Consequently, the folding and unfolding rates cannot be directly separated from the experimental kinetics. More rigorous approach is to develop models for the folding free-energy surfaces as functions of a suitable reaction coordinate, where protein folding is represented as stochastic, diffusive motion. Such low-dimensional free-energy surface picture provides a general framework for analysis of protein folding experiments and simulations [45–49], but its application is not without difficulties. Since the reaction coordinates are projections of multi-dimensional conformational space, the relevant folding steps correspond to complex combinations of many microscopic degrees of freedom. The folding motions are furthermore hindered by small activation barriers, typically smaller than k_BT and thus sometimes referred to as "microbarriers" [50]. Microbarriers originate from hindered rotations around the polypeptide backbone, steric clashes and breaking non-native interactions, often termed "surface roughness" [26]. The effective diffusion coefficient on the folding free-energy profile generally depends on the choice of the reaction coordinate [51], temperature and buffer conditions, and is expected to increase as the protein becomes more compact and approaches the folded state [50]. Interpretation of the kinetic folding experiments in terms of the underlying free-energy surfaces therefore requires characterization of the timescales of protein motions during all stages of folding, along with detailed understanding of their dependence on temperature, solvent properties and other experimental conditions.

The low-dimensional free-energy projections also provide means for reduction of the atomistic MD simulation data and common basis for the comparison of the microscopic simulations results with the macroscopic experimental kinetics. The reduced low-dimensional representation can be obtained from the full sets of kinetic rate equations by thorough statistical analysis of the corresponding structure of the associated rate matrix. As detailed below in Section 4, a working assumption is that a good definition of states adopted by a folding protein requires that the lifetimes in each configuration state are long enough such that transitions between states are essentially de-correlated. The implicit Markovian character of the folding dynamics can be thus captured fully by a rate matrix that can be ideally constructed from an exhaustive sampling obtained, for example, from atomistic level molecular simulations. In practice, it is often the case that the initially high dimensionality of the configuration space and, implicitly, of the rate matrix can be reduced significantly by clustering the states that are strongly connected. The development of methods that allow the systematic and even automatic clustering is an actively developing area [25,52–57]. Here, we present a method based on the eigenvalue and eigenvector analysis of rate matrices [25,58] that has the promise to offer a general framework that may be extended from the analysis of relatively small peptides to the folding of larger, more complex proteins.

3. Experimental studies of protein folding dynamics

3.1. Experimental methods

The main objective of the experimental protein folding studies is to relate the measurable, macroscopic kinetics to the microscopic dynamics and energetics of folding. There are two main classes of experimental approaches for studying the protein folding kinetics. The first are transient methods, where the equilibrium between the native and the denatured states is rapidly changed and the folding and/or unfolding transitions during the subsequent relaxation to the new equilibrium are followed. The second class is equilibrium methods, which follow fluctuations between the folded and unfolded

states under conditions where both are detectably populated. Measuring the folding kinetics in equilibrium requires monitoring a property that can be observed for the native and the denatured state without averaging. Both approaches depend on experimental probes that can reliably and with sufficient time resolution report on conformational states and transitions in the folding proteins.

3.1.1. Methods for monitoring protein structural changes during folding

Protein folding is generally followed using low-resolution spectroscopic methods. As these methods cannot directly determine the structure, they rely on the sensitivity to some structural feature, or, most commonly, structural change. Different experimental techniques may sense global, average structural content or local environment of the particular chromophore. Kinetic experiments can in principle detect the evolution of the macroscopic population of the folded or unfolded states in time. However, what is truly measured is the time dependence of the experimental signal, not the (un)folded structure. For the interpretation of the experimental folding data, it is therefore critical to understand the properties of the experimental method employed and the relation between the detected signals and structural changes in the studied protein.

Fluorescence is one of the most frequently used experimental methods for measuring protein folding kinetics [59]. The main advantages are high sensitivity and versatility; fluorescence can be employed in a number of different ways to monitor various characteristics of the protein structure. Most commonly, emission of the intrinsic tryptophan (Trp) provides information on the environment of this residue. Shifts in the fluorescence spectrum and changes in quantum yield are observed if the Trp buried inside the hydrophobic core of the protein becomes solvent exposed upon unfolding [60,61]. The fluorescence lifetimes, which are related to the fluorescence quantum yield, can also be directly measured [62–64]. Alternatively, quenching by other residue, such as protonated histidine (His), can be used to induce changes in the quantum yield of Trp and monitor the Trp-His contact [43,65,66]. Intrinsic fluorescence of tyrosine (Tyr) is occasionally used [67], although it is much weaker than that of Trp. Finally, an extrinsic fluorophore can also be engineered into the protein. The fluorescence lifetimes of the common chromophores are on the order of 1 nanosecond; therefore, fluorescence techniques typically allow investigating the dynamic processes with nanosecond time resolution.

Förster resonance energy transfer (FRET) allows measurement of intramolecular distances in proteins [68]. FRET experiments typically require modification of the protein by inserting a suitable FRET acceptor and/or donor chromophore. Intrinsic Trp, if present, often serves as a donor with several options for the acceptor. Using multiple FRET pairs, it is possible to measure several distances and their changes during protein folding, which can provide a detailed picture of the structure formation [69]. Furthermore, FRET can be used in single molecule experiments, to study distributions of distances during folding of individual protein molecules [9,70–72]. For single molecule FRET, suitable visible donor and acceptor chromophores must be engineered into the protein [73].

Infrared spectroscopy (IR) is another commonly used protein structural probe. IR reports on the protein secondary structure predominantly through the amide I band (mainly amide C = O stretch, 1600–1700 cm^{-1}), which is sensitive to the polypeptide backbone conformation due to characteristic couplings among the local amide modes [74]. Because of the interference of water (H_2O) vibrations, amide I is most commonly measured in D_2O solutions as amide I′ (N-deuterated). While only the average secondary structural content can be obtained from the standard IR spectra, site-specific resolution is possible with ^{13}C isotopic editing [75,76]. Moreover, the amide I is sensitive to the solvent exposure of the amide group and, therefore, tertiary environment [77,78]. IR methods can be used to investigate kinetic processes down to sub-picosecond time resolution. Millisecond time resolution can be achieved with standard Fourier-transform IR (FTIR) instruments [79], faster kinetics is most commonly measured at specific discrete frequencies using mid-IR lasers [80,81]. Spectrally resolved experiments are possible using ultra-fast, femtosecond lasers [82,83] and step-scanning FTIR [84]. Non-linear 2-D IR spectroscopy has also been applied to protein folding studies [85,86].

Raman spectroscopy, like IR, is sensitive to the protein secondary structure. In particular ultraviolet resonance Raman (UVRR) is a powerful method for measurements of the polypeptide conformational transitions [87,88]. UVRR takes advantage of specific resonance enhancement of the Raman scattering intensities for the amide backbone vibrations. Isotopic editing adds site-specific resolution to UVRR; especially the bending vibrations of deuterated C^{α}-H groups represent sensitive secondary structural probes complementary to the amide modes in the IR [89,90].

Circular dichroism (CD) in the far-UV region (180–250 nm) is most widely used to monitor the overall protein secondary structural content in equilibrium experiments. For kinetics measurements, the limitations of the CD arise mainly from the relatively low signal ($\sim 10^{-3}$ of the absorbance in the UV). UVCD experiments are commonly coupled with mixing (stopped flow) setup for initiation of folding or unfolding, which limits the time resolution to milliseconds (see below). Faster time-resolved far UVCD faces some experimental difficulties, but nanosecond time resolution has been achieved with this method in the visible, using suitable chromophores [91]. An alternative is the measurement of the optical rotatory dispersion (ORD), which is sensitive to the secondary structural changes in the near-UV and makes a time resolution of tens of nanoseconds possible [92]. Finally, magnetic circular dichroism (MCD) where the dichroism signal is induced by the magnetic field and generally much stronger than the natural CD, can be employed in some special cases [93].

Nuclear magnetic resonance (NMR) is perhaps the most versatile experimental technique, whose main advantage stems from the unparalleled spectral resolution. The structural information can be obtained from the chemical shifts, spin–spin coupling constants, residual dipolar coupling and cross-relaxation (nuclear Overhauser effect—NOE) signals [94,95]. The inherent timescales of the NMR spectral transitions are much longer than those for the optical methods. Structural changes in milliseconds or longer can be followed by NMR directly, using stopped-flow setup [94,95]. The comparable timescales of the protein and NMR spin dynamics, however, allow the NMR methods to sense a broad range of motions from picoseconds to milliseconds in equilibrium [96–98]. The high resolution of NMR also makes possible probing the dynamics of unfolded or partially folded states of proteins [99,100].

Hydrogen-deuterium exchange (HDX) is often combined with NMR but is not in itself a spectroscopic technique [101,102]. HDX is a chemical method, which allows labeling of the amide hydrogen atoms which are involved in hydrogen bonding, and therefore protected from exchange. Since the labeling can take place during the folding process, HDX can provide detailed, site-specific information about the evolution of protein structure. HDX can be used as a transient method by pulse labeling during protein refolding or in equilibrium. In pulse labeling, the H/D exchange is triggered and/or stopped by the change in pH at specific time delays after the refolding is initiated [101]. The protein is allowed to fully refold with the exchange quenched and the extent of exchange for individual amides is subsequently identified by 2D NMR, or mass spectrometry [103]. The fastest accessible timescales of pulse labeling are in the millisecond range, limited by the exchange kinetics and mixing times (see below). Equilibrium HDX takes advantage of the fluctuations of the protein between folded and unfolded states under varying denaturing conditions to characterize the metastable intermediate structures [101].

Many other experimental methods have been used to probe specific properties of proteins during folding. Some are less common, as they require very specialized resources. For example, small-angle X-ray scattering (SAXS), which provides information on the dimensions and the shape of the polypeptide chain [104–107], requires synchrotron X-ray source. Another example of a less commonly used technique is

photoacoustic spectroscopy [108]. Pulsed electron paramagnetic resonance (EPR) techniques in combination with spin labeling as well as liquid flow EPR have also been applied to investigate protein folding [109,110].

3.1.2. Transient techniques

3.1.2.1. Mixing methods. For decades, the workhorse of the kinetic protein folding experiments have been stopped-flow methods [111–114]. In stopped flow, mixing of two solutions, one of which contains the protein sample, abruptly changes the buffer conditions and thus shifts the equilibrium between the native and the denatured states. Usually, concentration of a chemical denaturant, typically urea or guanidinium hydrochloride (GndHCl), is changed, which can initiate both folding or unfolding if the denaturant is diluted out or its concentration increased, respectively. Additionally, the unfolding or refolding process can be triggered by change in pH, ligand concentration or temperature. To achieve rapid mixing, it is important to create highly turbulent flow conditions in a small volume to achieve a homogeneous mixture at molecular level. The design of the mixer varies from very simple T-arrangements to more complex mixing sphere setups [115]. The standard stopped-flow arrangements are limited by the mixing "dead time" to the time resolution of ~1 ms. Improvements to a submillisecond resolution appeared over the last several years [116]. The stopped-flow technique is usually combined with an optical device observing fluorescence emission, absorbance (UV through IR), or CD. Less commonly used probes are fluorescence lifetime measurements [62], NMR [95], and small-angle X-ray scattering (SAXS) [117]. Pulse labeling H/D exchange [101,102] also relies on rapid mixing, where following the denaturant dilution the exchange is initiated and quenched by pH jumps in additional mixing steps.

An improved time resolution over the stopped-flow methodology can be achieved with the continuous flow [118]. The continuous flow technique is also based on mixing of two different solutions but, unlike the stopped flow, the mixture is probed under steady-state flow conditions. By monitoring optical properties at different positions along the jet emerging from the mixer the kinetics can be measured via the direct relationship between the distance from the mixer and the reaction time. The dead times of continuous flow experiments are significantly shorter than those of the stopped-flow methods, ranging as low as 50 μs [118]. One of the disadvantages, however, is the large sample consumption. Recently, microfluidic mixing devices have been developed which can dramatically reduce the sample requirement but also the mixing dead time to several microseconds [119,120]. The microfluidic devices are typically combined with laser-induced fluorescence [119] to probe the protein folding but have been designed for use with other detection methods, such as synchrotron CD spectroscopy [121]. Furthermore, combination of rapid, microfluidic mixing techniques with the single molecule detection allows measuring the distributions of folding subpopulations under non-equilibrium conditions [122]. The time resolution of the single molecule mixing experiments, however, is limited to milliseconds or longer by the flow rate, whose increase results in the loss of the single molecule signal [123].

3.1.2.2. Temperature and pressure jump. The limitations of the mixing methods can be eliminated by the rapid perturbation of folding equilibrium using either temperature or pressure. The temperature jump (T-jump) can only increase the sample temperature. As a consequence, the equilibrium shift is toward the unfolded states, except when the protein can be cold denatured [13,124,125]. Pressure jump, on the other hand, can be applied in either direction: jumps to high pressures denature proteins, while rapidly reducing high pressure can trigger protein refolding [126,127].

Several different ways of inducing the temperature jump are possible. The classical method [128,129] uses a fast electrical discharge provided by a capacitor to rapidly increase the temperature of the electrolyte (buffer) by Joule heating. Temperature changes by 1–20 °C usually occur within 500 ns–10 μs depending on the experimental conditions [129]. Development of the pulsed laser initiated T-jump opened the possibility to trigger protein unfolding or refolding on nanosecond and even sub-nanosecond timescales. The laser T-jump methodology and its applications to investigations of biomolecular dynamics have been recently reviewed [130]. The most common experimental arrangement for laser T-jump is based on a nanosecond near-IR Nd:YAG laser, whose output is shifted further in the IR to be absorbed by an overtone of water or D_2O (for IR experiments). The absorbed energy directly heats the small volume of the sample by 10–20 °C over the time of the pulse duration, typically a few nanoseconds. The wavelength conversion is accomplished using Raman shifting [131,132], coherent mixing [133] or, more recently, by an optical parametric oscillator (OPO) [134,135]. The long time limit of the T-jump experiments is given by the cooling of the sample volume by thermal diffusion and is typically on the order of a millisecond [130]. Laser T-jump is therefore applicable to fast processes from nanosecond to microsecond ranges.

Protein folding is generally accompanied by a decrease in reaction volume and proteins unfold under pressure [126,127]. A sudden increase in pressure initiates protein unfolding, while for a pressure unfolded protein, the decrease in pressure triggers refolding. The pressure jump can be induced as repetitive pressure pulses by a stack of piezoelectric crystals [136] or as a single pressure jump using a mechanical valve [137]. Pressure jump measurements are possible over a wide range of temperature and solvent conditions and can follow the folding processes over a time range from ~100 μs to minutes [138]. The protein structural changes in response to the temperature or pressure jump can be monitored by several spectroscopic methods; the most commonly used is fluorescence, followed by IR.

3.1.2.3. Optical triggers. A rapid shift of the folding equilibrium can be caused not just by changes in the environment of the protein, but also in the protein molecule itself by photodissociation of a ligand, [139], electron transfer [140] or by specifically designed photoswitches [141]. In particular, small organic chromophores, also known as cages, can be employed as photolabile linkers. These phototriggers, such as a benzoin derivate linker, which constrains the protein in the unfolded state until it is photolyzed by a laser pulse [108], are attractive for folding studies, since refolding can be initiated from a relatively well-defined unfolded conformation. The same linker also allows triggering unfolding, rather than folding, under native conditions by blocking a destabilizing mutation [142]. Since the photolysis is fast (picoseconds) and irreversible, it is possible to measure processes lasting from picoseconds to seconds. The disadvantage of this molecular "staple", however, is that the irreversibility of the photolysis prevents averaging of multiple laser shots in order to improve the signal to noise ratio. Another example of a folding phototrigger is the photodissociable bond of aryl disulfide cross-linking group, whose cleavage by a laser pulse takes less than 100 ps [143,144]. The disulfide cross-linking is fully reversible, but it recombines in nanoseconds thus making impossible studies of slower processes. These limitations, along with the necessity to engineer the suitable linkers into the protein sequences, have so far prevented a more widespread use.

Another way to modulate the protein structural equilibrium is by using a linker that isomerizes upon illumination with light of a certain wavelength [85]. An azobenzene-based ultra-fast reversible photoswitch built into a 16-residue helical peptide used in combination with time-resolved IR spectroscopy was reported by Bredenbeck et al. [141] who achieved a time resolution of 2 ps and a long time limit of 30 μs. Another azobenzene-based photoswitchable linker was placed in the turn of a β-hairpin, where the *cis*-configuration initialized folding and the trans-configuration unfolding [145].

3.1.2.4. Mechanical force. The mechanical force can also serve as a denaturant by literally pulling apart single molecules of either large

proteins or smaller proteins artificially covalently linked into "polyproteins" [10,146]. The first method applied to study of the folding of single protein molecules under force, and still most commonly used, is atomic force microscopy (AFM) [147]. An alternative to AFM is the use of the optical tweezers [148], which offer less mechanical stiffness and reduced loading rates compared to AFM, and allow a more precise study of the folding or unfolding trajectories [149]. The unfolding is monitored as the increase in the polypeptide chain length. The force unfolding is carried out either with a stepwise or with a constant increase of the applied force (force-ramping) [150]. When stretched, protein refolding can be initiated by release of the pulling force. In contrast to other denaturing techniques unfolding by force does not always exhibit a reverse refolding without force. This provides access to parts of the free-energy landscape not accessible by classical unfolding methods. As a single molecule experiment, the technique offers the possibility of elucidating subpopulations of molecules sampling different pathways or rare intermediates [151,152].

3.1.3. Equilibrium techniques

Measuring kinetics of folding using equilibrium methods does not require fast initiation, but a significant population of both the folded and unfolded states must be present. The rates of interconversion can be measured either from incomplete averaging of the observed signal, if the timescale of the studied process is comparable to the intrinsic timescale of the experimental method (NMR), or by eliminating the ensemble averaging so that the equilibrium fluctuations between the folded and unfolded states can be resolved (single molecule methods). Typically, equilibrium techniques are applied to samples under denaturing conditions, at least mild, and the results have to be extrapolated to physiological conditions for very stable proteins.

3.1.3.1. NMR methods. NMR offers a wealth of experiments which can be tailored to probe a wide range of structural and dynamical properties. The NMR line broadening [153] has been among the first to identify the very fast folding proteins [154–156]. NMR line broadening is sensitive to the rates of exchange between two states, which have comparable difference in their respective resonant frequencies. Much faster exchange yields two sharp resonances, one for each state, while much slower exchange results in a single sharp peak due to the complete averaging. In the intermediate regime, the incomplete averaging significantly broadens the line shapes, to the point they may become almost undetectable. The exchange rate can be obtained directly from fitting the line shapes or, alternatively, from the transverse relaxation time, which is another measure of the line width [153]. Depending on the NMR field and chemical shift difference, the line broadening is sensitive to kinetics on the timescales of 10^{-4} to 10^{-1} s [153].

The NMR line broadening can be used to measure the folding kinetics from resolved methyl or aromatic ^{1}H resonances in one-dimensional (1-D) NMR spectra. A significant population of both the folded and unfolded states (>3%) is required. Relaxation dispersion techniques, in particular in combination with ^{15}N and ^{13}C isotopic labeling and two-dimensional (2-D) NMR detection, provide additional sensitivity (>0.5% population of the unfolded state) as well as site-specific information about the folding dynamics [97,98]. Relaxation dispersion experiments are powerful tools for studying protein folding in the millisecond range [157].

One of the limitations of the NMR methods is that the information about the dynamics is indirect. It is possible to extract rates of folding or unfolding from the relaxation or line broadening experiments, which are often in excellent agreement with those determined directly, e.g. by laser T-jump experiments. However, any deviations from simple kinetics, e.g. fast kinetic phases or non-exponential progress curves, which are extremely valuable for the protein folding studies, cannot be detected [67,158]. On the other hand, in combination with isotopic labeling the spin relaxation methods allow probing the kinetics with site-specific resolution. By monitoring the exchange rates for multiple resonances corresponding to the different amino acid residues, the deviations from the simple two-state behavior can be observed [97,159].

3.1.3.2. Single molecule methods. Conventional methods provide only an ensemble average of the measured properties over all molecules in the sample. Single molecule methods eliminate the ensemble averaging and instead of just a single, average value yield the true distributions of the molecular properties. Single molecule folding, aside from the mechanical force discussed above, is most commonly studied using Förster resonance energy transfer (smFRET) [9,71]. Since the FRET efficiency correlates to the donor-acceptor distance, it is possible to resolve different conformational subpopulations [10]. There are two main approaches to smFRET folding experiments. The simplest is detection of single protein molecules as they freely diffuse through the confocal volume [72,73,122]. The second approach is more technically demanding, but allows true watching the conformational fluctuations over time in individual protein molecules by tethering them to the surface [70,160,161]. FRET measurements on single immobilized molecules provide an alternative means to measurement of folding and unfolding rates from residence times in the extended and folded states as well as estimations of the folding transit time [161]. The single molecule methods have been limited by their detection timescales to milliseconds, but recent improvements in sensitivity have pushed this limit to submillisecond ranges and even made possible single molecule experiments on small, very fast folding proteins [162]. Furthermore, from the photon counting statistics or, alternatively, from the correlations of smFRET acceptor and donor intensities, the timescales of the protein reconfigurational dynamics in the unfolded states can be extracted [9,71].

Another method for monitoring dynamics on single molecule level, and nanosecond to millisecond timescales, is the fluorescence correlation spectroscopy (FCS) [163,164]. FCS measures the dynamics of stochastic fluctuations in fluorescence of protein molecules diffusing through the confocal detection volume. The autocorrelation function calculated from the time traces of the emission intensity contains information about all molecular events that contribute to the fluctuations in the fluorescence. These include the rates of diffusion through the detection volume, but also the conformational changes, such as folding or dynamics in the denatured states. To probe the conformational dynamics, typically a fluorophore and a quencher are engineered into the protein sequence [165–167]. Quenching of the fluorescence upon a van der Waals contact yields the rates of contact formation between the fluorescence and the quencher. FCS provides a sensitive tool for measuring conformational dynamics down to the nanosecond time regime.

3.2. Dynamics of elementary events in protein folding

As mentioned above, folding of many small, single domain proteins is limited by sizable free-energy barriers, which on one hand results in a simple experimental kinetics, but on the other prevents direct experimental investigation of the microscopic dynamics during folding. One way around the problem is to divide the folding process into elementary events, whose dynamic properties can be investigated using suitable model compounds [7,168]. At the most elementary level, the polypeptide conformational dynamics involves rotations around the polypeptide backbone dihedral angles. Combinations of many such individual transitions lead to formation of secondary structural elements, tertiary contacts by bringing specific segments of the protein into spatial proximity, and overall compaction of the polypeptide chains. Estimates of the timescales relevant for protein folding can therefore be obtained by kinetic measurements of folding of individual secondary structures, such as α-helices and β-hairpins, formation of disordered loops in oligopeptides and studies of the dynamics in denatured proteins.

3.2.1. Secondary structure formation

One of the essential events during folding of a protein is formation of the regular secondary structural elements, α-helices and β-structures. The kinetics of helix-coil transition in polypeptides was first investigated more than half a century ago using ultrasonic relaxation methods and found to occur in nanoseconds [169,170]. Only by late 1980s, however, have model oligopeptides become available that resemble the length and composition of α-helices found in proteins [171]. The nanosecond folding made the folding kinetics of model peptide helices ideal for applications of newly introduced laser T-jump methodology. Using IR [133], fluorescence [65] and UV resonance Raman [172] as structural probes, the laser T-jump experiments determined the folding times for the Ala-rich oligopeptide helices to be on the order of 500 ns. Like folding of many small proteins, the helix-coil kinetics resembles a simple two-state process due to the separation of timescales between the individual elongation steps and the barrier limited nucleation. Analysis of the experimental kinetics with the statistical mechanical model estimated the relaxation time of adding or removing the single residue from the helix at ~100 ps [65] and the nucleation barrier of ~3 k_BT. Two macroscopic rates were predicted: ~4 ns re-equilibration among the partially helical configurations and ~220 ns relaxation for the helix-coil transition, in excellent agreement with the biphasic kinetics observed in the IR experiments [133].

The detailed mechanism of the α-helix formation remains an intensely studied problem. Recent experiments revealed that folding thermodynamics and/or kinetics are probe-dependent [141,173,174] and the relaxation kinetics non-exponential [173–175]. In particular, laser T-jump combined with isotopically-edited IR [173,176,177] and UVRR [178], showed that individual isotopically labeled segments of the α-helix exhibit different relaxation kinetics. This implies a more complex folding mechanism than a simple, two-state transition. Huang et al. [173] proposed that the α-helix folds via a diffusive conformational search on a complex energy landscape. However, Doshi and Muñoz [179] have shown that this "complex" kinetics is in fact fully quantitatively consistent with the nucleation-elongation mechanism.

An important question is whether the Ala-rich peptides are realistic models for the α-helices in proteins. Gai and coworkers [180] found that the helix from the ribosomal protein L9 from *Bacillus stearothermophilus* exhibits a much slower T-jump relaxation kinetics, about 2 μs, than equivalent Ala-rich peptide helices. Much slower relaxation kinetics in stable, protein-like helices has been suggested due to higher entropic cost associated with the alignment of non-alanine side chains, and breaking of stronger side chain interactions [7]. However, bulky side chains were found to have no effect the α-helix folding kinetics in oligopeptides [181] and α-helices in proteins also appear to form on the same timescales as those in Ala-rich peptides [182].

Compared to the α-helices, peptide models for the β-sheet structure presented more of a challenge, predominantly due to their tendency to aggregate. A suitable model was found in the C-terminal β-hairpin from the GB1 protein [183]. From laser T-jump experiments, the GB1 β-hairpin folding time was found to be ~6 μs [184], an order of magnitude longer than that of the α-helix. The β-hairpin folds much slower due to a significant entropy barrier, which arises because non-local inter-residue contacts must form. Since long-range contacts are a general feature of protein structures, folding of a β-hairpin closely resembles that of larger, single domain proteins. A simple statistical mechanical model used for the analysis of the β-hairpin folding kinetics [185] also proved to be remarkably successful when applied to the folding of small proteins [48,186]. For these reasons, and for its simplicity, the GB1 β-hairpin has become one of the paradigm models for theoretical studies of the folding mechanism [187–193].

More recently, other β-hairpin peptide models have appeared, such as tryptophan zippers (trpzips), stabilized by two pairs of Trp residues, whose folding kinetics has been intensely studied using laser T-jump methods [194–197]. Investigation of several trpzips suggests that the turn formation is the rate-limiting factor in β-hairpin folding, consistently with the model for the GB1 hairpin. Comparison of trpzip4 with GB1, which diverge in their sequence only in the hydrophobic cluster, shows very similar folding times (~15 and ~6 μs, respectively) although the unfolding rates were found to differ significantly (~234 and ~6 μs) [195].

The kinetics and mechanism of folding for larger, three- and four-stranded β-sheet peptides has also been investigated [198,199]. Both the three-stranded and the four-stranded β-sheet exhibited a surprisingly high folding rate (~0.44 μs at the thermal melting temperature). The folding kinetics of the four-stranded β-sheet supports the suggested dependence of the folding rate on the number of β-strands by increasing the folding barrier by 0.8 kcal/mol compared to a three-stranded β-sheet [198]. The folding was described by an apparent two-state model although there are probably parallel kinetic pathways involved [199].

3.2.2. Dynamics in unstructured peptides

Another essential step in protein folding is the formation of tertiary contacts, which requires bringing to close proximity amino acid residues distant in the polypeptide sequence. Rates of contact formation in unstructured model oligopeptides were investigated by several research groups and different experimental approaches: fluorescence quenching [200], FRET [201], triplet-triplet energy transfer (TTET) [202] and triplet quenching [203,204]. The timescales of the contact formation differ somewhat depending on the particular method, peptide sequence and conditions. Overall, the Gly-Ser [205] and Ala-Gly-Asn [203] repeat sequences form loops of 6–10 residues, the most common loop lengths in proteins, within 15 to 60 ns. The loop formation rates in Gly-Ser repeat sequences are only weakly dependent on single amino acid substitutions, with flexible Gly yielding the fastest, and stiffest trans-Pro the slowest rates [205]. For short loops, the rates are also only weakly dependent on length, due to the dominating effect of chain stiffness. For longer loops ($\gtrsim$ 20 residues), the length dependence of the loop closure time approaches that expected for the ideal Gaussian chain [206] $\tau_C \propto n^{3/2}$ [203,205]. Krieger et al. used these values to estimate the value of the pre-exponential factor in Eq. (1) to be on the order of 10^8 s^{-1} [205]. However, this estimate is likely to be several orders of magnitude too high, as discussed in greater detail in Sections 3.3.3 and 3.3.4.

Huang and Nau [200] studied the end-to-end contact rates for tetra- and hexapeptides of all 20 amino acids as a measure of the conformational flexibility. For the hexapeptides, the rates ranged from 25 ns (Gly) to ~400 ns (Ile), with Pro too slow to be measurable. The rates correlate well with the side chain size, indicating lower conformational flexibility. In particular, the β-branched amino acids were found to be among the most rigid. The charge repulsion in protonated Asp, Glu and Lys was also found to slow down the rate of contact formation.

The kinetics of end-to-end, end-to-interior and interior-to-interior loop formation were compared by Fierz et al. [207]. The rate of end-to-interior loop formation decreased with increasing chain length to a limiting factor of 2.5-fold slower than end-to-end loop formation. The analysis of the length dependence suggested that the rate is determined by the ratio of loop length to the total length of the peptide. The rate of interior-to-interior loop formation is slower by an additional factor of 1.7 [207]. These results indicate that the local motions of the peptide chains are strongly coupled, with those closer to the termini exhibiting faster dynamics. The loop closure rates for the same loop sequences but different tail lengths showed the same viscosity dependence, which argued against increased solvent–peptide interactions causing the slower dynamics. Local steric effects of the additional tails, which could potentially restrict the accessibility of the interacting groups, were also found an unlikely cause for the different dynamics. Fierz et al. therefore concluded that the differences in the loop formation kinetics for the three types of loops was caused by the inherent flexibility between various positions in the chain.

Additional studies explored the effects of denaturants on the peptide dynamics [201,205,208] The GndHCl in general slows the

end-to-end contact formation in peptides considerably, in contrast to the effect on the dynamics in denatured proteins, which is discussed in the following section. This is due to expansion of the chain in denaturant, which effectively increases the mean diffusion distance for the ends to collide. It is possible that more compact peptide conformations also form intramolecular hydrogen bonds [201]. The transition from essentially length independent contact rates to the Gaussian chain dependence occurs for shorter peptide lengths in denaturant, indicating higher chain flexibility under high denaturant conditions [205].

3.2.3. Dynamics in unfolded proteins

Our understanding of the properties of unfolded state has been limited mainly due to the experimental difficulties associated with the structural heterogeneity of the unfolded ensembles. Furthermore, investigations of the unfolded states usually have to be carried out under at least mildly denaturing conditions to ensure the unfolded states are detectably populated. However, the most physiologically relevant and therefore interesting for studying protein folding are native conditions. Such experiments require that the unfolded subpopulations can be resolved and separated from the folded states, which has become possible in particular using single molecule methods.

Gopich et al. [209] investigated the dynamics of the unfolded states of cold shock protein Csp*Tm*, using single molecule FRET (smFRET) and varying concentration of denaturant (GndHCl), from 8 M GndHCl to essentially zero. From the FRET acceptor and donor intensity autocorrelation functions the reconfiguration times for the polypeptide chain have been determined to be ~20 ns at high denaturant concentration (8 M GndHCl) and ~65 ns under native conditions. The rate of end-to-end contact formation (~1 μs^{-1}) is within the rates of contact formation in unstructured model oligopeptides extrapolated to the same length. The effective end-to-end diffusion constants are also very similar to those for the short peptides [210], suggesting that the denatured proteins are flexible. Consistently, in a related study [211], multi-site FRET found isotropic distributions of distances in Csp*Tm* and no evidence for native-like topology in the unfolded states under low denaturant conditions.

The reconfiguration time τ_r is directly related to the rate prefactor in Eq. (1). Using Kramers' theory (Eq. (3)) and assuming the frequency factors and the diffusion constant in the unfolded well and on the barrier top are equal [212]:

$$\tau_0 = \frac{1}{k_0} = \frac{2\pi k_B T}{\omega_0^2 D_0} = 2\pi\tau_r \tag{4}$$

which yields $\tau_0 \approx 0.4$ μs for $\tau_r \approx 65$ ns under the native conditions. The faster reconfiguration time at high denaturant concentration reflects the decrease in the underlying free-energy "roughness" or, equivalently, increase in the effective diffusion coefficient, due to more expanded chain and weakened intrachain interactions by the denaturant. However, the change in k_0 is essentially negligible, compared to the nine orders of magnitude decrease in the folding rate $k_F = k_0(1/P_F - 1)$ between 0 M and 8 M denaturant for this protein (here P_F is the folding probability). This illustrates that the denaturant predominantly affects the free-energy barrier by shifting the folding equilibrium, and also highlights the importance of the unfolded state dynamics studies for estimating the dynamic timescales in folding.

Somewhat slower contact formation was found for a small 44-residue domain BBL using single molecule fluorescence correlation spectroscopy (FCS) by Fersht and coworkers [167]. The BBL domain was destabilized by mutation to ensure detectable population of the unfolded state under native condition. The fluorescence autocorrelation function of extrinsic fluorophore oxazine, which is efficiently quenched upon contact by tryptophan engineered into the BBL sequence, revealed several distinct processes. The submicrosecond decay was assigned to the contact formation in the unfolded states, the ~10-μs phase to folding and the slow millisecond decay to the diffusion through the detection volume. The contact formation time was found to be 500 ns, which is several fold slower than the rates of contact formation in the model oligopeptides [203,205], and in Csp*Tm* [209,210]. Furthermore, the rate was found independent on the loop length in two BBL variants with the quencher (Trp) 35 and 25 residues apart from the oxazine fluorophore [167]. The differences were attributed to the intrachain interactions and/or lower flexibility compared to the model peptides. However, no such effects were observed for the dynamics of the unfolded Csp*Tm* [209,210] or for the collapse of the BBL domain measured using laser T-jump [135], discussed in the next paragraph.

By contrast, residual intrachain interactions support the observation of significantly slower unfolded state dynamics in several other proteins, such as RNAseH, which was investigated by smFRET on surface immobilized proteins [160]. The reconfiguration time for this protein was estimated as 20 μs from the acceptor-donor cross correlation function even at high denaturant concentration (6 M GndHCl). The Gaussian chain model, however, yielded the lower bound to the reconfiguration time of 170 ns. Single molecule FCS study of the dynamics in intestinal fatty acid binding protein (IFAPB) [166] revealed the apparent relaxation time of the conformational fluctuations ~1.6 μs at 3.5 M GndHCl, significantly longer than that estimated for the Gaussian chain. The relaxation slowed down with increasing viscosity, suggesting a diffusion limited process. The relaxation was slower (~2.5 μs) in a molten globula state at pH 2, further increasing with the amount of salt-induced secondary structure. Like the kinetics of the α-helix folding above, it still remains a question whether the dynamics of the unfolded chains of proteins occurs on the same or slower timescales than that of the unstructured peptides.

3.2.4. Hydrophobic collapse

The compaction of the polypeptide chain is an important step in the protein folding process, in particular when the solution conditions are changed from denaturing to native [213]. The collapse may occur concurrently with [214] or precede [215,216] the formation of native structure. Experimental studies of the collapse transitions are difficult due to competition with folding under native conditions, while chemical denaturants weaken the hydrophobic driving forces. Single molecule methods again offer a distinct advantage owing to their capability to resolve the unfolded subpopulations even under essentially native conditions.

The kinetics of the hydrophobic collapse was first studied in cytochrome *c* under mildly denaturing conditions using laser T-jump and Trp fluorescence as a probe [217]. The ~100-μs collapse kinetics was found to be a two-state activated process with an apparent activation energy of ~5 kcal mol^{-1}. More recently, Muñoz and coworkers [135] investigated the hydrophobic collapse without chemical denaturants for an acid denatured small protein BBL. The spectrally resolved fluorescence laser T-jump setup monitored FRET between the ends of the protein. The collapse relaxation was found to be much faster, ~60 ns at 305 K, and with no evidence for the activation barrier. At low temperatures, the relaxation kinetics follows the temperature dependence of the solvent viscosity, indicating that it is a diffusive process with no activation energy. At higher temperatures the collapse slowed down, as a consequence of the decrease in the effective diffusion coefficient due to stronger hydrophobic effect.

The compaction of the denatured proteins is evident from the equilibrium distributions of end-to-end distances in *sm*FRET experiments. The unfolded distribution generally shifts toward lower values with decreasing denaturant [73]. Single molecule studies of the collapse dynamics, however, support both barrier limited and diffusive barrier-less collapse. In RNAseH immobilized on the surface, so that the individual transition events could be followed in real time, very slow barrier limited dynamics within the denatured ensemble been found with the time constant of ~2 s [160]. The barrier height

was estimated from the measured reconfiguration time of 20 μs to be 10 k_BT and attributed to preorganized structure and intramolecular interactions. By contrast, the nanosecond collapse dynamics in Csp*Tm* [194], which falls within the range of dynamic timescales measured for short disordered peptides, points toward absence of any specific interactions and energy barriers. Similarly, barrier-less collapse was reported by the smFRET study of the immunoglobulin G binding domain of protein L [218].

The nanosecond collapse times measured in denatured proteins should be considered only as lower limit of the collapse transition [213], since they correspond to only a small change in the overall chain dimension. The collapse during folding, on the other hand, should be a large-scale, non-equilibrium transition in which the chain attains essentially the size of the folded state. Attempts to study the hydrophobic collapse with rapid mixing devices using FRET [216] or SAXS [104,219] to monitor, respectively, the end to end distance or radius of gyration, can only set an upper limit around a few hundred microseconds [213] for the collapse uniformly takes place during the dead time of the measurements. The timescales of the protein hydrophobic collapse along with its role in the folding process therefore still remain an unresolved problem.

3.3. Dynamics during folding

The studies of model compounds and denatured proteins have provided important insights into the timescales of the intramolecular polypeptide chain dynamics. As with the secondary structure formation and dynamics of the unstructured chains, the important question is whether these timescales correspond to those in actual proteins. As some of the above discussed examples indicate, the dynamics in proteins may be significantly slower [160,166,167,180], especially as the folded state is approached [50]. These problems can be addressed by studies of proteins which fold over marginally small free-energy barriers or even "downhill" in free energy. In such "ultra-fast" folding proteins and particularly in the limit of no free-energy barrier, the dynamics of the re-equilibration among the partially folded populations can be directly experimentally observed [8].

3.3.1. Ultra-fast folding and non-exponential kinetics

In protein folding, ultra-fast refers to microsecond or faster folding times, approaching the rates of the elementary events, discussed above. Within the last decade, a number of ultra-fast folding proteins have been identified [16,220]. Experimental studies of such proteins are well beyond the time resolution capabilities of the mixing methods, and have been carried out predominantly using laser T-jump techniques. Most of the ultra-fast folders are small α-helical proteins, either naturally occurring domains or *de novo* designed sequences. However, several all β-sheet WW domains [221,222] also fold ultra-fast, as do some α/β proteins [223]. In fact, the fastest folding rate to-date has been record for a β-sheet structure [198].

In many ultra-fast folding proteins the relaxation kinetics is bi-exponential with the two phases often well separated in timescales [41,43,67,224–226]. The bi-exponential kinetics suggests either intermediates, re-equilibration among the partially folded states as in the α-helix-coil transition or, possibly, the signature of the "molecular" diffusive dynamics. Furthermore, the folding kinetics is often dependent on the particular experimental probe used to monitor the structural changes. These characteristics can provide important clues about the mechanism of the folding process. An example is one of the most intensely studied small α-helical domains, a three helix bundle B-domain of protein A (BdpA). The folding kinetics was first studied using NMR line broadening in the presence of denaturant and the folding rate of ~10^5 s^{-1} (folding time of ~10 μs) was determined by extrapolation to the native conditions [155]. The NMR, however, cannot follow the fast folding kinetics in real time, in particular detect the additional kinetics phases. By contrast, laser T-jump experiments revealed a very fast ~80 ns relaxation in addition to the microsecond transition [67]. Relative amplitudes of the ~80 ns and the microsecond phases in the IR amide I′ signatures of the buried and solvent exposed α-helices, as well as site-specific fluorescence probes [67], led to a clear picture of the folding mechanism. The middle α-helix of BdpA forms rapidly, followed by the cooperative folding of the other two helices together with the tertiary structure, consistently with the protein engineering studies [227].

The BdpA example demonstrates the utility of measurements of the real-time fast folding kinetics, in particular within the nanosecond time range. It also shows that the kinetics, in this case the relative amplitudes of the individual macroscopic phases, may depend on the experimental probes. Consequently, simple exponential kinetics measured with one particular experimental probe does not necessarily guarantee simple kinetics behavior overall. Finally, the knowledge of the characteristic timescales for folding of α-helices, elucidated from the experiments on model peptides, provides important clues as to the origins of the additional, very fast kinetic phases.

Similar biphasic kinetics were observed for another ultra-fast folding protein, the 35-residue villin headpiece subdomain (HP-35) independently by the fluorescence (an N27H variant, N = Asn, H = His, with the His introduced as a Trp quencher, providing a fluorescence probe for folding) [43] and IR experiments [228]. The ~70-ns kinetic phase was interpreted as re-equilibration within the folded well, since the amplitude was maximum at low temperatures with high folded state populations. Moreover, due to the placement of the fluorescence probe on the C-terminal helix, the fast phase was tentatively assigned to the partial unfolding of this helix. This explanation was supported by additional experimental evidence [229], statistical mechanical modeling [230] and simulations [231]. Very recently, using TTET Kiefhaber and coworkers reported a ~1-μs unlocking transition in the native state of HP-35, where the individual α-helices cooperatively break from the hydrophobic contact [232]. The unlocking leads to the transient unfolding of the C-terminal helix with the relaxation time of 170 ns. This observation is consistent with the observed biphasic T-jump relaxation kinetics and proposed folding mechanism of this protein. The TTET study also found that GndHCl denatured HP-35 shows identical behavior to unstructured peptides, implying the residual native structure in the unfolded state is not the reason for ultra-fast folding.

Different explanation of fast kinetic phases was proposed by Gruebele and coworkers [225,233,234], who studied an ultra-fast folding variant of the λ-repressor by laser T-jump experiments. The wild type of λ_{6-85} folds in ~250 μs via an apparent two-state process, but stabilizing mutations accelerate folding to ~20 μs. An additional, ~2 μs relaxation observed for the ultra-fast folding variant was interpreted as the diffusional dynamics on the folding free-energy surface, which directly corresponds to the pre-exponential factor k_0 in Eq. (1). The "molecular phase", as the fast kinetic phase is termed, has been detected in other proteins as well [235]. Observation of the molecular phase is the signature of low barrier, as it arises from the population in the activated region that folds "downhill" in free energy. The amplitude of the fast phase increases with the bias toward the native state [236], which is consistent with the decrease in the folding barrier height, and scales inversely with solvent viscosity, as expected for a diffusional process (Eq. (3)). In the limit of no barrier, the activated phase vanishes and only the molecular phase is observed, which may further deviate from a simple exponential by becoming "stretched", i.e. of the form $\exp(kt^{\beta})$, where $\beta<1$. The stretched, or "strange" kinetics was predicted in the energy landscape theory of folding as a consequence of the kinetic traps or, equivalently, free-energy surface roughness [26]. Stretched T-jump relaxation kinetics was observed in α-helical peptides [174–176] (see above) as well as in proteins [13], and assigned as the downhill folding phase. In addition, the kinetics, as well as the folding thermodynamics, of the ultra-fast folding λ_{6-85} depends on whether it is followed by fluorescence or IR [234], a signature of non-cooperative folding. To support the interpretation of the experimental folding data, Gruebele

and coworkers used folding simulations by Langevin dynamics on empirical one-dimensional free-energy surfaces [41,225,234,237]. The surfaces predict the biphasic, non-exponential and probe-dependent kinetics when the folding is essentially downhill in free energy. While these simulations can reproduce well the observed kinetics, they do not necessarily exclude other solutions [238].

3.3.2. Experimental signatures of barrier-less folding

The signatures of the downhill folding remain a controversial problem. Deviations from a mono-exponential relaxation, in particular stretched kinetics [13], which reflects a distribution of different rate processes, was proposed as one possible characteristics. Kinetics dependent on the particular experimental structural probe, corresponding to non-cooperative sequential or gradual process, is another possibility. However, simulations of folding as diffusion on low-dimensional free-energy surfaces demonstrated that both barrier limited or downhill folding can lead to either exponential or non-exponential and probe-dependent kinetics [238]. Simulations have also shown that virtually any realistic folding scenario leads to exponential kinetics [239]. Non-exponential and probe-dependent kinetic are thus unreliable signatures of barrier-less folding.

Gruebele and coworkers proposed that the downhill folding is revealed if the protein is "stressed" [41], i.e. destabilized, by temperature, solvent conditions or mutations. The stressing results in "tuning" of the free-energy barrier, which leads to the characteristic changes in the experimental folding kinetics. This is supported by additional studies on the λ-repressor, which could be tuned from a two-state to a downhill folder, where the kinetics changes from a single exponential (slow "activated" phase) to bi-exponential for low barrier, to only the "molecular" phase (~2 μs) [236]. The molecular phase can be exponential or stretched, if the diffusion is not simple, and dependent on the experimental probe. The transition from downhill to two-state folding under thermal stress was demonstrated for a number of mutated λ_{6-85} variants [240].

Muñoz argued that barrier-less folding will be identified as gradual, non-cooperative process by probe dependence of the unfolding thermodynamics [241,242]. Using multitude of experimental methods, the Muñoz group showed that the variant of a small peripheral subunit binding protein BBL folds globally "downhill" [243]. Global downhill folding in which there is no free-energy barrier to folding under any, even highly destabilizing, conditions is the Holy Grail of the folding studies, since unfolding results in the gradual shift of populations toward the unfolded state. In such scenario, the intermediates can be observed under equilibrium conditions. A particularly noteworthy experiment is the thermal unfolding of the BBL monitored by NMR for hundreds of protein resonances [244]. This study found that virtually each proton thermally unfolds through a distinct transition. Sanchez-Riuz and Muñoz also developed a method for estimation of the free-energy barriers from the unfolding heat capacity profiles, measured by the differential scanning calorimetry (DSC) [245], which revealed a unimodal, barrier-less folding free energy. While model dependent, the estimations show good correlation with the kinetic data, especially for fast folding proteins [246], and with barrier height estimations from the rate theories and statistical mechanical models [247]. The laser T-jump folding kinetics of BBL was also recently reported, monitored by IR and FRET [80]. Both probes show exponential relaxation with common relaxation times of 1.3 μs at 333 K, but an order of magnitude slower (20 μs) at low temperature, indicating a relatively rough underlying energy landscape.

The global downhill folding of the BBL domain was, however, from the onset challenged by Fersht and others [162]. Recently, Fersht and coworkers were able to follow the GndHCl unfolding of the BBL using smFRET [248]. While at the limit of detectability due to the microsecond folding–unfolding, with increasing denaturant the smFRET could resolve two distinct distributions of FRET efficiencies. The two populations are a characteristic of two macroscopic states, at least as probed by the FRET acceptor–donor distances, and were observed for two-state proteins, such as Csp*Tm* [73]. By contrast, the global downhill or one-state protein is expected to have just one detectable population, which should gradually shift between the folded and unfolded. Single molecule experiments may therefore represent the most direct criterion for distinguishing between one- or two-state folding. It appears that BBL does not fold globally downhill with respect to GndHCl denaturation. This, however, does not mean that the BBL could not behave as a downhill folding protein without denaturant. Bimodal smFRET distance distribution was reported for another ultra-fast folder BdpA [162], where, however, the bi-exponential kinetics also points toward the existence of a free-energy barrier.

3.3.3. Protein folding "speed limit"

The maximum rate at which the protein can fold without the free-energy barrier is another possible criterion for the identification of downhill folding. The concept of speed limit is based on the notion that when the bias toward the native state is increased, the maximum rate of protein folding is achieved when the barrier to folding first disappears. Further increase in the native bias may not further accelerate folding, since stronger stabilizing interactions are expected to increase the surface roughness (frustration) and decrease the effective diffusion coefficient.

The question of the folding speed limit was first invoked by Hagen and Eaton [15], who proposed a generic value of the maximum folding time of ~1 μs, based on the collapse rates in denatured cytochrome *c*. Subsequently, with fast kinetic data available for the timescales of the elementary events in folding, unfolded chains and ultra-fast folding proteins, the problem of the speed limit was revisited. Using the available data, theoretical estimates and scaling arguments from the polymer theory, Kubelka and Eaton [16] proposed the minimum folding time for an *N*-residue protein to be $\tau_{\text{limit}} \approx N/100$ μs. Comparison with the folding rates of known proteins, which were empirically normalized to different stabilities and lengths, suggested that most ultra-fast folders can be engineered to fold considerably faster. Indeed, stabilization of the villin headpiece subdomain HP-35 N27H by double mutation resulted in the record breaking rate of ~700 ns [66]. However, the relaxation kinetics was still biphasic, reflecting the timescale separation due to the free-energy barrier. The residual free-energy barrier height was estimated from the Kramers' theory (Eqs. (1) and (3)) to be $\lesssim 1$ kcal mol^{-1}, indicating that further stabilization is required to eliminate the barrier and further supporting the speed limit estimate.

The above speed limit estimate only depends on the length of the protein. The argument for the linear scaling is that on the downhill folding surface the folding time will be proportional to the number of diffusion steps along the reaction coordinate, which is commonly the number of ordered (native) residues. It is clear, however, that additional factors will affect the folding speed limit for specific protein sequences. In particular, the α-helical proteins are expected to fold faster than those containing β-sheets. More recently, Muñoz and coworkers [249] analyzed the ultra-fast kinetic data of nine proteins using a one-dimensional free-energy surface model. The analysis indicated that one of the ultra-fast folders, the albumin binding domain, is a globally downhill folding protein, while several others, including the wild-type HP-35, fold downhill at room temperature (298 K). The minimum folding times at the unfolding midpoint temperature were calculated in the vicinity of 2 μs, with the exception of HP-35 N27H (0.5 μs) and Pin WW domain (10 μs). Owing to the strongly temperature dependent effective diffusion coefficient, a significant increase in the minimum folding time was predicted at 298 K, ranging from about 2-fold to more than a factor of 50. It is not clear whether the results are not simply a consequence of the assumptions and parameters of this simple model. In particular, only the overall folding rates and their temperature dependence were modeled, with no attempt to fit the kinetic amplitudes or additional kinetic phases. Especially peculiar is the significant difference in the predictions for the two variants of HP-35,

which experimentally show very similar behavior [43,228]. However, an important point is that the intrinsic dynamical timescales in proteins can be significantly different. Proteins with high barriers in some cases can fold faster than others that are downhill and the dynamics, rather than free-energy barriers can significantly contribute to the temperature dependence of the folding rates.

3.3.4. Solvent viscosity and internal friction in folding dynamics

From the above discussion it appears that the maximum rates of protein folding are considerably lower ($k_0 \sim 10^6\ s^{-1}$) than those observed in diffusion limited contact formation in peptides (e.g. estimate $k_0 \sim 10^8\ s^{-1}$ of Krieger et al. [205]). Folding of the peptide α-helices is also faster than the estimated folding speed limits, despite the fact that α-helices and ultra-fast folding proteins cross comparable free-energy barriers [179]. The limits to folding rates are thus set by the dynamics, or the effective diffusion coefficient in the energy landscape view. According to Kramers' theory (Eqs. (1) and (3)), the folding time is proportional to friction, which, to the first approximation is given by the solvent viscosity: $\tau_F \propto 1/k_F \propto \eta$. However, additional contribution to the effective friction is expected to arise from the polypeptide chain itself [250], so that $\tau_F \propto \eta + \sigma$. The "internal" friction σ arises from hindered bond rotations, steric clashes, breaking of non-native interactions and other processes that dissipate energy in the reaction coordinate [251]. The contribution of the internal friction is likely to be significant especially in compact structures, as indicated, for example, by the dynamics of collapse discussed above [135,209].

Interestingly, some proteins show no evidence of internal friction: for example, for the IgG-domain of *peptostreptococcal* protein L the viscosity dependence of the folding time extrapolated through zero for $\eta \to 0$ [252]. Hagen et al. [251] argued that the associated timescale, rather than the internal viscosity per se, should be the measure of its contribution to the folding dynamics. For millisecond and slower folding proteins, the effects in micro- to nanosecond ranges would be undetectable. On the other hand, the internal viscosity effects should stand out for very fast folding proteins. Significant contribution of the internal viscosity was detected for two microsecond folders: the ferrocytochrome *c* folding from a highly compact, collapsed state [253], and the *de novo* designed miniprotein tryptophan cage (Trp cage) [254]. The extrapolated zero viscosity folding time for the ferrocytochrome *c* was 8 μs (293 K), compared to 12 μs in water. The internal friction is therefore a dominant factor in determining the folding rate of this protein from the compact late stage intermediate. Furthermore, the extrapolated zero viscosity folding times are strongly temperature dependent, indicating a large enthalpic contribution. By contrast, for the Trp cage the extrapolated folding rates are temperature independent, which is consistent with diffusive, entropic search for the folded state. On the other hand, for the unfolding times, a significant activation enthalpy was found, as expected due to breaking stabilizing interactions [254].

The internal friction is expected to increase as the protein approaches the folded state, where the structures are more compact and a higher number of intrachain interactions formed. Recently, Cellmer et al. [255] studied the effects of solvent viscosity on the folding kinetics of HP-35 N27H villin headpiece subdomain. These authors used ethylene glycol as viscogen, which was found to have no effect on the protein stability; adding denaturant to ensure isostability conditions was therefore unnecessary. The folding kinetics was modeled by diffusion on a 1-D free-energy surface calculated from a statistical mechanical model based on the folded structure. The model could explain the data with the internal friction constant linearly increasing as a function of the number of native contacts, used as the reaction coordinate. The overall change in the effective diffusion coefficient, however, was relatively small, decreasing by a factor of 10 or less. Interestingly, an increase in the internal friction was found for increasing temperature, somewhat in contrast to the estimations by Muñoz and coworkers [249]. However, the experiments and modeling were carried out only at high temperatures (50–70 °C) and it is therefore not clear how the internal friction scales down to the room temperature. Since an increase in the strength of the hydrophobic effect at high temperature was suggested as one of the possible explanations [255], it is possible that the temperature dependence of the internal friction is non-monotonic and may start to decrease at lower temperatures, as observed for an acid denatured BBL [135]. An alternative explanation for the internal friction increase is the shift of the transition state with temperature towards the native structures, predicted by the model free-energy surface, where the chain dynamics becomes more restricted [255]. Finally, the solvent viscosity and internal friction may have even more pronounced effects on protein folding, such as altering the folding pathways, as indicated by both experiments [256] and simulations [257].

4. Protein folding kinetics from molecular dynamics simulations

Molecular dynamics (MD) simulations present an alternative method for investigating the intricate details of folding processes that can complement the experimental observations. However, there are major problems that limit the usefulness and the applicability range of simulations. In a nutshell, computer simulations of folding are limited by their *efficiency*, *accuracy* and, last but not least, *methodology*.

The most obvious problem is *efficiency*: how much statistical data can be generated for a certain molecular system. While this used to be the major problem in the past, current molecular simulations can benefit dramatically from Moore's law. Recent all-atom simulations have been used on systems as large as the entire ribosome [258]. A second aspect affecting the efficiency is the resolution of the molecular model being used. While *ab initio* quantum calculations are still prohibitively expensive for most systems of biological interest, classical atomistic MD remains the norm. Recent years have seen a renewed interest in simplified (i.e., coarse grained) models that often consider the interaction with water as implicitly included in a minimal representation (e.g., one interaction center per residue) of peptides and proteins [4].

The *accuracy* is mainly affected by the choice of interaction parameters, and therefore largely independent of simulation length and system dimensions. Being independent on computational hardware, accuracy cannot be improved by simply taking advantage of Moore's law, and thus the quest for force fields with better interaction parameters is likely to remain central to MD simulations research for years to come. While most atomistic force fields with explicit solvent seem to provide a reasonable agreement with (at least global, macroscopic) experimentally measurable quantities (e.g., folding populations, J-couplings, etc.) [23], improvements are still needed. As mentioned above, it would be crucial in protein folding to obtain agreement between atomistic MD simulation and experimental observations in terms of the microscopic, local structural transformations that control the specific folding–unfolding mechanisms (i.e., pathways and populations of intermediates, kinetic traps, etc.).

Finally, advances in *theoretical* and *algorithmic methods* for studying protein folding can both alleviate problems affecting efficiency and accuracy, as well as evolve the understanding of protein folding processes in general and thus bridge the current gaps between experiments and computational simulations. While both experiments and simulations are evidently affected by their intrinsic sources of errors, certain errors such as those related to methods used to define and discretize the configuration space or to estimate the transition rates from time series could benefit significantly from a systematic theoretical framework [25,52–55,259]. On the algorithmic side, recent years have seen a dramatic development and use of advanced simulation methods such as replica exchange, simulated tempering, STMD, metadynamics, etc. [12,260–265]. In particular, promising new methods such as the ones presented below, based on a Markovian assumption about the character of transitions between the configuration states and their associated propagators, also offer a systematic method for analyzing and describing the way in which peptides and proteins navigate their typically complex free-energy surfaces [25,52–57,266].

4.1. Coarse master equations: a theoretical framework for protein folding dynamics

Master equations of the coarse configuration space dynamics [267–275] provide a rigorous theoretical framework that can be used to address in a systematic and quantitative manner both the kinetic aspects of protein folding that are relevant to experimental observations, as well as the increasingly complementary data offered by molecular simulation methods. Their utility comes from the basic possibility to map the typically complex kinetic processes involved in protein folding on a reduced (thus "coarse") representation that would capture accurately the relevant relaxation timescales and folding–unfolding probabilities. The various limitations of projecting molecular kinetics, which occurs on intrinsically complex free-energy landscapes, on coarse-grained low-dimensional reaction coordinates has long been recognized and analyzed in detail [269,276–278]. In the master equation formalism, in close connection to kinetic rate theories for barrier crossing, the protein folding dynamics is modeled as an intrinsically stochastic process in which the molecules explore their energy landscape by following a sequence of transitions (or "jumps") between their various kinetic states (or "cells"). The statistical configuration space of proteins or other biomolecules is thus mapped using the coarse master equation (CME) approach on a low-dimensional manifold consisting of a kinetic network of states that are metastable compared to the timescales characteristic to inter-state transitions. For Markovian-like dynamics (i.e., for systems with rapidly decaying memory with regards to the specific sequence of transitions between their states) the probability of observing the system in a configuration state n at a certain time t, denoted by $p_n(t)$, depends on the connectivity between state n and its neighboring states (e.g., m). The variation in time of the probability of state n is related to the rates of transition between m and its connected neighbor states m through a flux balancing relation known as the master equation

$$\frac{dp_m(t)}{dt} = \sum_{n=0}^{N-1} [k_{mn}p_n(t) - k_{nm}p_m(t)] \tag{5}$$

where k_{mn} is the rate of transitions from state n to state m, and N is the total number of states. Using the vector–matrix notation, Eq. (5) becomes simply

$$\frac{d\mathbf{p}}{dt} = \mathbf{K}\mathbf{p} \tag{6}$$

where $\mathbf{K}$ is the square rate matrix of size N, and $\mathbf{p}$ is a column vector of time-dependent probabilities $p_n(t) > 0$, $n = \{0,1,...,N-1\}$.

The stationary equilibrium distribution on a fully connected kinetic network of configuration states is given by

$$\mathbf{K}\mathbf{p}^o \equiv 0 \tag{7}$$

which is normalized such that $\sum_{n=0}^{N-1} p_n^o = 1$ and positive $p_n^o > 0$, $n = \{0,1,...,N-1\}$. The elements of the square rate matrix $\mathbf{K}$ have the property

$$k_{nm} = \begin{cases} -\sum_{i=0\,(i\neq n)}^{N-1} k_{in}, & n = m \\ k_{mn}p_n^o / p_m^o, & n > m \end{cases}. \tag{8}$$

The definition of the rate matrix (8) ensures that local equilibrium is attained through the detailed balance relation

$$k_{nm}p_m^o = k_{mn}p_n^o. \tag{9}$$

4.1.1. Spectral properties of the rate matrix

Beyond brevity, an important advantage of the matrix formulation of master equations is that it allows the use of powerful spectral analysis methods to study the intrinsic kinetic properties of a system described by a certain rate matrix $\mathbf{K}$. As required by the condition of unique stationary equilibrium (Eq. (7)), one of the eigenvalues is zero, and all others are real and negative.

In general, the non-symmetric rate matrix $\mathbf{K}$ has distinct right and left eigenvectors φ_i and χ_i, respectively, that satisfy the corresponding eigenvalue equations

$$\mathbf{K}\varphi_i = \lambda_i\varphi_i, \text{ and } \chi_i\mathbf{K} = \lambda_i\chi_i. \tag{10}$$

In the following, we assume that the eigenvalues are sorted by magnitude: $\lambda_0 = 0 > \lambda_2 \geq \lambda_3 \geq \cdots \geq \lambda_{N-1}$.

Motivated by both theoretical and computational reasons, we discuss the eigenanalysis of the rate matrix $\mathbf{K}$ by introducing the symmetrized rate matrix $\mathbf{H}$ defined as

$$\mathbf{H} \equiv \mathbf{P}_o^{-1/2}\,\mathbf{K}\,\mathbf{P}_o^{1/2} \tag{11}$$

where $\mathbf{P}_o = diag[p_0^o, ..., p_{N-1}^o]$ is the diagonal matrix of equilibrium probabilities such that its trace is $tr(\mathbf{P}_o) = 1$.

The elements of the symmetrized rate matrix $\mathbf{H}$ are given by [58]:

$$h_{nm} = \begin{cases} k_{nn} = -\sum_{i=0\,(i\neq n)}^{N-1} k_{in}, & n = m \\ \sqrt{k_{nm}k_{mn}}, & n \neq m \end{cases}. \tag{12}$$

The symmetrized rate matrix $\mathbf{H}$ has eigenvalues λ_i with corresponding orthonormal eigenvectors such that

$$\mathbf{H}\psi_i = \lambda_i\psi_i \tag{13}$$

Note that the matrix $\mathbf{H}$ has the same eigenvalues λ_i as the original $\mathbf{K}$ matrix and analytically related eigenvectors. Moreover, the left and right eigenvectors of the $\mathbf{K}$ matrix are obtained from the corresponding elements of the eigenvectors of the symmetrized rate matrix as the product of the squared eigenvector elements of $\mathbf{H}$ with the corresponding equilibrium probability values, such that

$$\begin{aligned} \varphi_i(n)^2 &= p_n^o \cdot \psi_i(n)^2, \\ \chi_i(n)^2 &= \psi_i(n)^2 / p_n^o \end{aligned} \tag{14}$$

and $\varphi_i(n)^2 = (p_n^o)^2 \cdot \chi_i(n)^2$.

It follows from Eq. (7) that the first right eigenvector of the original matrix $\mathbf{K}$ (i.e., the one corresponding to the eigenvalue $\lambda_0 = 0$) is given by the equilibrium population, $\varphi_0(n) = p_n^o$ and, correspondingly, $\chi_o(n) = 1$, for any $n = 0,1...,N-1$. Using Eq. (14) one then finds that

$$p_n^o = \psi_0^2(n), \forall n \in \{0, 1..., N-1\}. \tag{15}$$

From the orthonormality of the ψ_n eigenfunctions one obtains the normalization conditions

$$\begin{aligned} \sum_{n=0}^{N-1} \psi_i(n)\psi_j(n) &= \sum_{n=0}^{N-1} \chi_i(n)\chi_j(n)p_n^o \\ &= \sum_{n=0}^{N-1} \varphi_i(n)\varphi_j(n) / p_n^o = \sum_{n=0}^{N-1} \varphi_i(n)\chi_j(n) = \delta_{ij} \end{aligned} \tag{16}$$

where δ_{ij} is the Kronecker delta function. Consequently, we have

$$\sum_{n=0}^{N-1} \psi_i(n)\sqrt{p_n^o} = \sum_{n=0}^{N-1} \chi_i(n)p_n^o = \sum_{n=0}^{N-1} \varphi_i(n) = \delta_{0i}. \tag{17}$$

As shown next, these relations are central to the computational investigation of the dynamics of kinetic systems such as protein folding.

4.1.2. Evaluating relaxation timescales with correlation functions and propagators

The rate matrix symmetrization presented above allows the convenient treatment of the formal solution of the coarse master Eq. (6), which can be rewritten using the matrix $\mathbf{H}$ as

$$\frac{d\boldsymbol{\pi}}{dt} = \mathbf{H}\boldsymbol{\pi}, \tag{18}$$

where we use the mapping

$$\boldsymbol{\pi} = \mathbf{P}_o^{-1/2}\mathbf{p}. \tag{19}$$

The solution of Eq. (6) is thus given conveniently in terms of the eigenvalues and eigenvectors of the symmetric matrix $\mathbf{H}$ as

$$p_n t = p_n(0)\sum_{i=0}^{N-1}\psi_i^2(n)\exp(\lambda_i t) \tag{20}$$

for any $n \in 0,1...,N-1$.

Interestingly, the mapping on a symmetrized dynamics allows us to express any correlation function in terms of the eigenvalues and eigenvectors of matrix $\mathbf{H}$. For example, the autocorrelation function of any time-dependent observable $\mathbf{a}(t)$ projected on the N states of the system can be written as

$$\langle \mathbf{a}(t)\mathbf{a}(0)\rangle = \sum_{i=0}^{N-1}\left[\sum_{n=0}^{N-1} a_n\psi_0(n)\psi_i(n)\right]^2 \exp(\lambda_i t). \tag{21}$$

In general, $\mathbf{a}(t)$ can be any function depending on the discrete conformational state function of the system denoted by $s(t) \in \{0,1...,N-1\}$.

Note that for the particular case when $\mathbf{a}(t) = \psi_i(s(t))/\psi_0(s(t)) = \chi_i(s(t))$, we find that the autocorrelation function of $\mathbf{a}(t)$ is given by

$$\left\langle \frac{\psi_i(s(t))}{\psi_0(s(t))}\cdot\frac{\psi_i(s(0))}{\psi_0(s(0))}\right\rangle = e^{\lambda_i t}. \tag{22}$$

Eq. (22) is central to a particularly useful procedure for finding the eigenvalues of a Markovian dynamic system by monitoring the decay of the autocorrelation functions calculated for the projections of the $\mathbf{H}$ eigenvectors on the $s(t)$ trajectory. In conjunction with the expression for the propagator, we have

$$G(n,t\,|\,m,0) = \left[e^{\mathbf{K}t}\right]_{nm} = \frac{\psi_0(n)}{\psi_0(m)}\sum_{i=0}^{N-1}\psi_i(n)\psi_i(m)\exp(\lambda_i t) \tag{23}$$

where the Green's function $G(n,t|m,0) \equiv G(n,t|m,t_0=0)$ is defined as the conditional probability that the system is in state n at time t, given that it was initially in state m at time $t_0 = 0$.

Finally, we emphasize that the ability to estimate correctly the propagators of a Markovian system is crucial to our analysis of protein folding trajectories as they are required by the computation of the likelihood function for molecular trajectories obtained directly from simulations. For any trajectory of a Markovian system we express its likelihood function as

$$\Lambda = \prod_{i=1}^{N_{\text{int}}} G(s(i\Delta t),\Delta t\,|\,s((i-1)\Delta t),0) \tag{24}$$

where the trajectory is divided uniformly in the N_{int} number of intervals of equal time length Δt, the total time of a simulated trajectory being $t_{\text{total}} = N_{\text{int}}\Delta t$. Considering the Markovian character of the dynamics, if $T_{nm}(\Delta t)$ is the total number of transitions that take a trajectory from state m to state n after a lag time Δt, the likelihood to observe this trajectory can be written [25] as

$$\Lambda = \prod_{n=0}^{N-1}\prod_{m=0}^{N-1}\left[G(n,\Delta t\,|\,m,0)\right]^{T_{nm}(\Delta t)}. \tag{25}$$

Eqs. (23) and (25) provide the formal connection between the number of transitions observed in an MD simulation trajectory and the intrinsic transition rates that dictate the dynamics. The maximum likelihood value for Λ (or equivalently the minimum value of $-\log(\Lambda)$) could be attained by optimizing our estimation of the elements of the rate matrix $\mathbf{K}$ for an observed number of transitions collected in the transition matrix $\mathbf{T}$.

4.2. Sampling the configuration space

The rate analysis methods described above, either based on likelihood maximization or on correlation functions, rest on the assumption that the entire configuration space of the system can be identified and sampled with a good accuracy. The limited sampling problem remains one of the major obstacles in using molecular simulations to study biomolecules. However, the methods for extracting rates from molecular trajectories do offer a systematic way to evaluate the quality and the convergence of the sampling results. For this reason, the first systematic studies of rate extraction were performed on relatively short polyalanine peptides (e.g., Ala_2, Ala_5, etc.) for which the conformational space spanned by all the possible combinations of Ramachandran angles can be sampled exhaustively. For example, each residue in the capped alanine pentapeptide, presents its own well-known free-energy surface in Ramachandran coordinates.

Fig. 1 illustrates this energy landscape (ΔG) for MD simulations using the Amber-GSS all-atom force field with explicit TIP3P water molecules [12,25]. While in general there are obvious differences along the sequence, in this simple case the features of the free-energy landscapes remain essentially the same for different residue numbers. For alanine residues, the main feature of these landscapes is the presence of a well-defined α-helical basin. Therefore, one can approximate the configuration space of a residue as consisting of two states: α-helical and non-α-helical. Thus, for pentaalanine, a $2^5 = 32$ state initial size of the conformational space can be used to enumerate all the possible combinations. Also shown in Fig. 1 is a sample trajectory for one residue that crosses between its α-helical and non-α-helical states. Note that this represents just a potential low-dimensional projection of the inter-state trajectory of the entire pentaalanine molecule as it travels between its 32 possible conformations [25]. Also shown are possible conformational boundaries that could be used in a conformation-based assignment of states. If only the α-helical minimum and its neighboring barriers are used, the simplest black square boundary could be used to separate the two states on the Ramachandran map. A better state assignment could be done by using also information about the presence of the second (β-sheet) minimum, using thus the red circular boundaries depicted in Fig. 1. In both cases, however, a purely conformational-based assignment (CBA) of states for a given trajectory would lead to the well-known problem of the occurrence of transition boundary "re-crossings" that could be easily misidentified as actual conformational transitions.

To address this concern, one can use a transition-based assignment (TBA) of states, where history about the states visited by a molecular trajectory is also used in addition to conformational information in order to assign a certain instantaneous conformation of a molecule to its proper kinetic configuration state [25]. The TBA procedure is illustrated in Fig. 2 for a typical 1D trajectory for which it is possible to identify with high confidence the values of a certain reaction coordinate that would correspond to each of the two states S1 and S2 (e.g. folded and unfolded). In practice, it is often possible to identify (e.g., by simple conformational averaging) reaction coordinate values that correspond to the two free-energy minima and to define

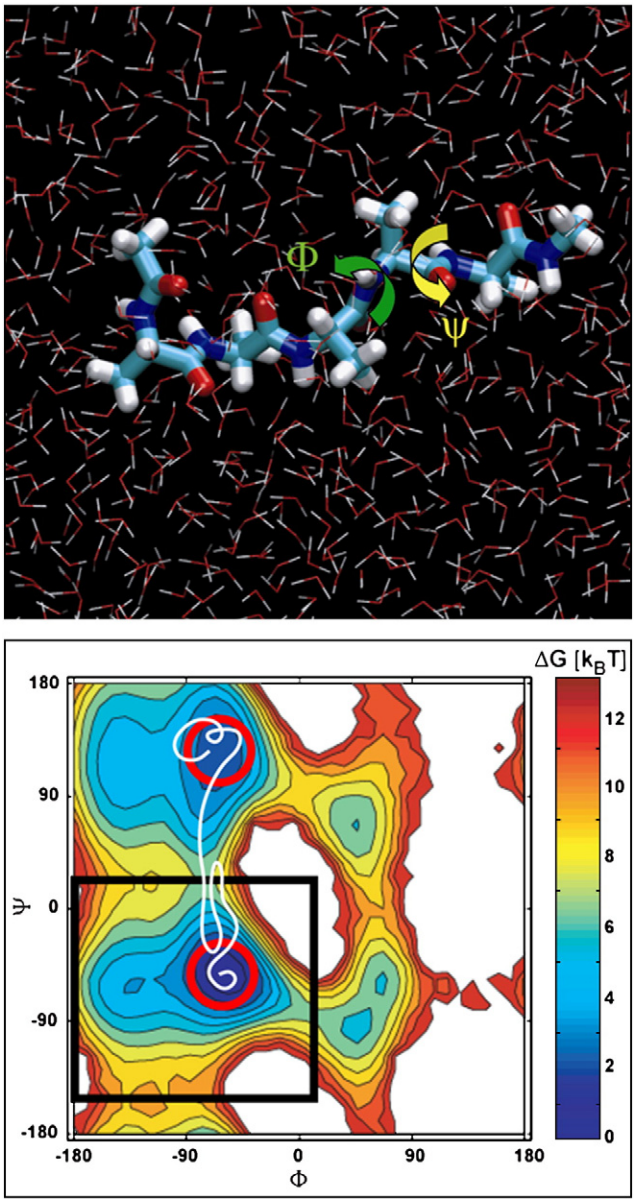

Fig. 1. Ramachandran angles and a representative Ramachandran free energy map for an alanine residue in pentaalanine, modeled with an all-atom Amber-GSS force field and explicit TIP3P water molecules. A possible trajectory (white curve) crosses in and out of α-helical regions. The features of this energy landscapes are used in the conformation-based (CBA) and transition-based (TBA) assignment of configuration states for each alanine residue.

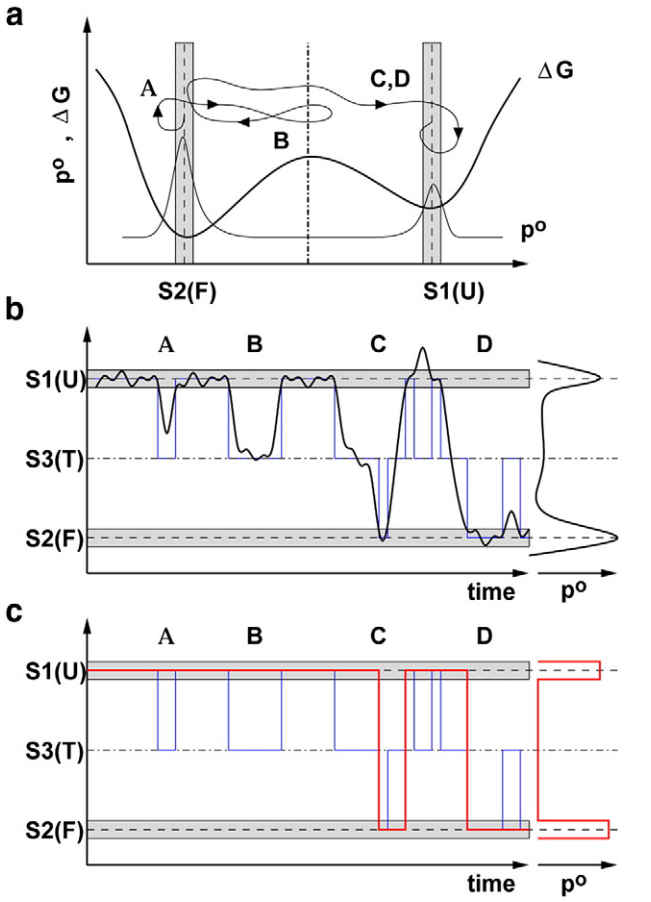

Fig. 2. Schematic representation of state assignment of a two-state trajectory. A typical conformation-based assignment (CBA) Kramers' approach uses a single (transition state) boundary, located on or near the top of the barrier and searches for corrections of the transition rate that estimate the effect of re-crossings. In contrast, a transition-based assignment (TBA) Markovian approach on using history information, relies on estimating first the location of the centers of the two-state manifolds and using narrow regions (gray) to define relatively narrow reaction coordinate ranges near the well bottoms that can be used to assign states. These regions are used in a first step (b) to assign instantaneous conformations along a trajectory to the well-defined two states together with a third "temporary" state. Finally, in a second step (c) the "temporary" state is eliminated based on the history of the conformational trajectory (see text and [25]).

relatively narrow regions (depicted as gray in Fig. 2a) around those minima that correspond to the two target states.

In the first step, conformations are assigned based only on conformational (geometric) characteristics by using the boundaries of these two narrow regions. The states outside the "gray" regions are assigned at this first stage to a "temporary" fictional state that would consist of states, re-crossings, as well as transition paths. After this first step, the continuous trajectory (see Fig. 2b) becomes a discrete trajectory including one extra state "S3" (blue line). This state is finally eliminated in a second trajectory analysis step (see Fig. 2c) by using the TBA method that takes into account the past and future history of the trajectory in the S3 regions. Thus, if both past and future states neighboring a temporary S3 region are identical, the S3 states are assigned to this corresponding state. However, if the past and future neighboring states differ, the S3 segment can be assigned to either of them. For a time-reversible state assignment, the first half of the S3 segment can be assigned to the past and the second half to the future conformation [25]. Also shown in Fig. 2 are possible examples of trajectory segments that are only short non-reactive excursions that enter and exit of the narrow S1 and S2 regions (noted A, B and D) as well as actual transition paths (e.g., in the C region).

4.3. Extracting kinetic transition rates from simulation trajectories

As mentioned above, Eqs. (23) and (25) provide a robust formal connection between the number of configuration transitions observed in a typical MD simulation trajectory and the intrinsic transition rates that dictate the actual dynamics of a certain biomolecular system. Alternatively, if the quality of the sampling is converged, the more typical method to obtain the elements of the rate matrix is by statistical analysis of lifetime distributions for each configuration state [25]. Both the propagator-based (PB) method presented here and the more common lifetime-based (LB) method of estimating rates are equivalent to each other in the limit of infinite sampling. However, the actual LB and PB estimated rates could vary significantly for simulations that do not benefit from a sufficiently long exploration of the entire space of configurations [25,279]. While the results of the LB method are affected mainly by the number of observed transitions between states and, thus,

by the total simulation time of a given system, the rates estimated with the PB method are also affected by the length or the observation windows (a.k.a., lag time) used for estimating the propagator values from the molecular simulation trajectories. At the same time, as illustrated in the previous section, both methods depend also on the accuracy of the procedure used for assigning the instantaneous configurations visited by the system to actual kinetic states.

The lag-time dependence of the rates extracted with the PB method presents the further advantage of offering a systematic way to explore these effects on the accuracy of the MD extracted rates. In the limit of infinitely small lag times, for identical trajectories (yet sufficiently converged), both the LB and PB methods give the same results. However, as the lag time values approach the intrinsic relaxation times scales of the optimal rate matrix **K**, the PB values become more accurate and less sensitive to the accuracy of the state assignment. As the propagator lag times increase further above the relaxation timescales intrinsic to the system being investigated, errors introduced by the limited sampling become especially important for long-time propagators and the accuracy of the PB-extracted rates decreases again [25].

The advantages of using a PB method for extracting rates as opposed to the more commonly used LB methods using lifetime distributions becomes apparent, as it offers a systematic way of targeting the rate-extraction procedure towards higher accuracy. Moreover, in certain cases such as simulations based on short trajectories, lifetime distributions are not even available. A typical case is rate extraction from protein folding simulations using the replica exchange molecular dynamics (REMD) method, where trajectories at a certain temperature are often interrupted because of the accepted exchange events. Nevertheless, since short lag time propagators can still be estimated, the PB method allows the estimation of accurate transition rates even for the increasingly popular REMD studies [12].

Methods such as the PB-based rate extraction coupled with the TBA method of assigning conformational states in folding–unfolding trajectories are one example of the recent methodological advances that could eliminate to a great extent the ubiquitous artifacts due to more or less arbitrary definitions of kinetic states and their boundaries. Other significant steps in this direction were already made in analyzing single-molecule time series [280,281]. These studies represent just a few of the recent excellent examples [259,282,283] in which network descriptions of protein folding are used for kinetic analysis, with the goal of making proper connection with experiments. At the same time, it is worth emphasizing that the problem of properly assigning configuration states to a certain molecular trajectory remains of central importance as it is directly related to Kramers' barrier re-crossing issues and, therefore, it can affect the results of estimating lifetimes and, implicitly, transition rates. The transition-based state assignment [25] presented above offers a systematic method to control and minimize the errors due to a certain conformation-based state assignment. Recent alternative methods based on automatic clustering of states [53,54,284] or on analyzing inherent structures [285] also lead towards a similarly systematic Markov analysis of folding–unfolding trajectories. Thus, it appears that different more or less independent approaches can reveal the underlying folding free-energy landscape and its associated kinetic network of configuration states and converge towards a systematic and unbiased description of protein dynamics [53,282,285].

4.4. Analyzing coarse-grained projections of folding kinetics

Arguably, one of the most important consequences of being able to estimate the full rate matrix **K** for a certain protein folding system is the ability to infer its minimal representation that is able to capture its characteristic intrinsic dynamics. For many systems using an atomistic level representation, the dimensionality of the entire configuration space (and thus of the rate matrix) **N** is typically extremely large, much larger than current analysis methods can handle. Therefore, there is an increased interest in clustering together states that are intrinsically connected by fast transition rates, as being part of the same extended configuration basin. This clustering represents in fact an effective coarse graining of the protein folding–unfolding dynamics under study, and several methods are available [25,52–54]. For properly defined basin boundaries, the transitions between configuration basins are typically orders of magnitude slower than intra-basin relaxation processes and are reflected in gaps observable in the eigenvalue spectrum of a rate matrix **K** that is initially very detailed and thus high dimensional.

The typical example is the kinetics of an effective two-state protein for which there is a significant separation between the value of its first (i.e., non-zero) eigenvalue λ_1 and the rest of the spectrum (i.e., $\lambda_2/\lambda_1 >> 1$, with $\lambda_0 = 0$). In this case, the quantities of interest are mainly the slowest inter-basin relaxation rate and the boundaries (and thus the populations) of the two basins. This information can be easily derived by eigenvalue analysis of the rate matrix **K**. Recent work has shown that the corresponding eigenvectors of the rate matrix **K** can be used to effectively assign the different configuration states to each basin, preserving both the basin populations as well as the slow relaxation rates [25,52,54]. In particular, for two-state proteins, the elements of the eigenvector corresponding to the largest non-zero eigenvalue are directly correlated to values of the folding probability of the system (i.e., the probability that the system would fold first before reaching the unfolded basin) [286]. This powerful observation offers an excellent approximation for calculating the folding probability, for identifying transition states and for analyzing the folding–unfolding kinetics in many practical cases [25,286,287].

5. Summary and outlook

Understanding the dynamics of protein amino acid chains is essential for uncovering the mechanism by which proteins fold. The rapidly growing interest in the protein folding problem among many different scientific disciplines has led to a considerable wealth of experimental and theoretical information on the dynamics of folding. The sheer volume of the available data makes an exhaustive review of all the contributions and literature related to the dynamics of protein folding all but impossible; in the above, we attempted to highlight the most important current issues on selected examples, in particular in areas closest to our own expertise.

On the experimental side, the most important contributions have come from fast, laser-triggered methods, which extended the available time resolution beyond the millisecond dead time limit of the traditional stopped-flow experiments. The data on the kinetics of formation of the secondary structure elements and inter-residue contacts have established an important basis for estimation of the intrinsic timescales involved in folding. The nanosecond time resolution is also critical for studying the kinetics of the ultra-fast folding proteins, in particular for following the “complex” kinetics and fast phases, which provide important additional information about the folding process. Secondly, single molecule techniques have provided critical information on the dynamics of the polypeptide chains, particularly in denatured proteins, that is not available to the ensemble experiments.

Application of these methods to a variety of systems, including oligopeptide models and a number of different proteins, indicates that the characteristic dynamics timescales may differ considerably. It is therefore likely that the protein dynamics may not be universal but dependent on the particular protein sequence and its related structural and energetic properties. In what lies ahead, the focus should therefore shift on the residue- and sequence-specific effects in folding. The use of multiple independent spectroscopic probes, which report on different structural properties, will be essential to gain detailed structural insights into the dynamic processes. In this respect, the isotopically edited IR or UVRR spectroscopies, which provide structurally non-perturbing, site-specific markers of the local

backbone conformation and solvation, and can be adapted for ultra-fast folding experiments, are especially promising. Reliable interpretation of the experimental spectral signals in terms of the protein structural changes is another area that will require further attention as different experimental probes often reveal distinct and even contradicting results. In hand with the more specific experimental probes, it will also be necessary to implement new methods for the data analysis. The low-dimensional free-energy surfaces have proven to be very powerful in this respect. However, it will be necessary to move beyond empirical *ad hoc* free-energy profiles and those treating all residues in the same, "averaged" manner and incorporate residue-specific properties. Relating the experimental data through the free-energy surfaces to the energetics of the individual protein amino acid sequences will lead to the understanding of general principles that govern folding of specific, individual protein sequences. It will also be necessary to model the observable spectroscopic signals based on their physical properties and in relation to the specific protein structures rather than by using arbitrary "dividing surfaces".

Ultimately, the most detailed interpretation of the folding experimental data in terms of the microscopic mechanism will have to come from theoretical folding simulations. As the modeling quality of current atomistic force fields converges, new methods that allow an automatic and, ideally, exhaustive analysis of the typically complex kinetics of peptides and proteins are highly needed. To capture the essential intrinsic dynamical feature of folding biomolecules, the new methods will likely have to span various levels of detail in a systematic and theoretically consistent manner. The stochastic kinetic analysis methods based on coarse master equations presented in this paper are promising candidates for fulfilling these theoretically challenging demands.

Acknowledgements

We thank Drs. A.M. Berezhkovskii, W.A. Eaton, J. Hofrichter, G. Hummer, and A. Szabo (NIH, NIDDK, LCP, Bethesda, MD) for many helpful and stimulating discussions. G.S.B. and R.D.M. have contributed equally to this paper. This research used the computational resources of the Irish Centre for High-End Computing (ICHEC). The authors gratefully acknowledge the financial support by the Irish Research Council for Science, Engineering & Technology (IRCSET) to R. D.M. and N.V.B and by the National Science Foundation (NSF CAREER 0846140) grant to J.K.

References

[1] D. Kennedy, C. Norman, What don't we know? Introduction, Science 309 (2005) 75-75.
[2] C.M. Dobson, Protein folding and misfolding, Nature 426 (2003) 884–890.
[3] Y. Zhang, Progress and challenges in protein structure prediction, Curr. Opin. Struct. Biol. 18 (2008) 342–348.
[4] N.V. Buchete, J.E. Straub, D. Thirumalai, Development of novel statistical potentials for protein fold recognition, Curr. Opin. Struct. Biol. 14 (2004) 225–232.
[5] A. Liwo, M. Khalili, H.A. Scheraga, Ab initio simulations of protein folding pathways by molecular dynamics with the united-residue (UNRES) model of polypeptide chains, FEBS J. 272 (2005) 359–360.
[6] R.H. Callender, B.R. Dyer, R. Gilmanshin, W.H. Woodruff, Fast events in protein folding: the time evolution of primary processes, Annu. Rev. Phys. Chem. 49 (1998) 173–202.
[7] W.A. Eaton, V. Muñoz, S.J. Hagen, G.S. Jas, L.J. Lapidus, E. Henry, J. Hofrichter, Fast kinetics and mechanisms of protein folding, Annu. Rev. Biophys. Biomol. Struct. 29 (2000) 327–359.
[8] W.A. Eaton, Searching for "downhill scenarios" in protein folding, Proc. Natl. Acad. Sci. USA 96 (1999) 5897–5899.
[9] B. Schuler, W.A. Eaton, Protein folding studied by single-molecule FRET, Curr. Opin. Struct. Biol. 18 (2008) 16–26.
[10] A. Borgia, P.M. Williams, J. Clarke, Single-molecule studies of protein folding, Annu. Rev. Biochem. 77 (2008) 101–125.
[11] M. Shirts, V. Pande, Screen savers of the world unite! Science 290 (2000) 1903–1904.
[12] N.V. Buchete, G. Hummer, Peptide folding kinetics from replica exchange molecular dynamics, Phys. Rev. E 77 (2008).
[13] J. Sabelko, J. Ervin, M. Gruebele, Observation of strange kinetics in protein folding, Proc. Natl. Acad. Sci. USA 96 (1999) 6031–6036.
[14] S.J. Hagen, Exponential decay kinetics in "downhill" protein folding, Proteins Struct. Funct. Gen. 50 (2003) 1–4.
[15] S.J. Hagen, J. Hofrichter, A. Szabo, W.A. Eaton, Diffusion-limited contact formation in unfolded cytochrome *c*: estimating the maximum rate of protein folding, Proc. Natl. Acad. Sci. USA 93 (1996) 11615–11617.
[16] J. Kubelka, J. Hofricheter, W.A. Eaton, The protein folding 'speed limit', Curr. Opin. Struct. Biol. 14 (2004) 76–88.
[17] J. Mittal, R.B. Best, Dependence of protein folding stability and dynamics on the density and composition of macromolecular crowders, Biophys. J. 98 (2010) 315–320.
[18] D. Tsao, A.P. Minton, N.V. Dokholyan, A didactic model of macromolecular crowding effects on protein folding, PLoS ONE 5 (2010) 8.
[19] H.J. Dyson, P.E. Wright, Intrinsically unstructured proteins and their functions, Nat. Rev. Mol. Cell Biol. 6 (2005) 197–208.
[20] A.L. Fink, Natively unfolded proteins, Curr. Opin. Struct. Biol. 15 (2005) 35–41.
[21] A.K. Dunker, I. Silman, V.N. Uversky, J.L. Sussman, Function and structure of inherently disordered proteins, Curr. Opin. Struct. Biol. 18 (2008) 756–764.
[22] N.V. Buchete, J.E. Straub, D. Thirumalai, Orientation-dependent coarse-grained potentials derived by statistical analysis of molecular structural databases, Polymer 45 (2004) 597–608.
[23] R.B. Best, N.V. Buchete, G. Hummer, Are current molecular dynamics force fields too helical? Biophys. J. 95 (2008) L7–L9.
[24] R.B. Best, G. Hummer, Optimized molecular dynamics force fields applied to the helix-coil transition of polypeptides, J. Phys. Chem. B 113 (2009) 9004–9015.
[25] N.V. Buchete, G. Hummer, Coarse master equations for peptide folding dynamics, J. Phys. Chem. B 112 (2008) 6057–6069.
[26] J.D. Bryngelson, J.N. Onuchic, N.D. Socci, P.G. Wolynes, Funnels, pathways, and the energy landscape of protein folding—a synthesis, Proteins Struct. Funct. Gen. 21 (1995) 167–195.
[27] J.N. Onuchic, Z. Luthey-Schulten, P.G. Wolynes, Theory of protein folding: the energy landscape perspective, Annu. Rev. Phys. Chem. 48 (1997) 545–600.
[28] S.E. Jackson, How do small single domain proteins fold? Fold. Des. 3 (1998) R81–R91.
[29] R. Zwanzig, Two-state models of protein folding kinetics, Proc. Natl. Acad. Sci. USA 94 (1997) 148–150.
[30] M. Karplus, Aspects of protein reaction dynamics: deviations from simple behavior, J. Phys. Chem. B 104 (2000) 11–27.
[31] D.J. Bicout, A. Szabo, Entropic barriers, transition states, funnels, and exponential protein folding kinetics: a simple model, Protein Sci. 9 (2000) 452–465.
[32] S.S. Plotkin, J.N. Onuchic, Understanding protein folding with energy landscape theory—part I: basic concepts, Q. Rev. Biophys. 35 (2002) 111–167.
[33] R.B. Best, G. Hummer, Coordinate-dependent diffusion in protein folding, Proc. Natl. Acad. Sci. USA 107 (2010) 1088-1093.
[34] S.V. Krivov, M. Karplus, Diffusive reaction dynamics on invariant free energy profiles, Proc. Natl. Acad. Sci. USA 105 (2008) 13841–13846.
[35] B. Qi, S. Muff, A. Caflisch, A.R. Dinner, Extracting physically intuitive reaction coordinates from transition networks of a beta-sheet miniprotein, J. Phys. Chem. B 114 (2010) 6979–6989.
[36] H.A. Kramers, Brownian motion in a field of force and the diffusion model of chemical reactions, Physica 7 (1940) 284–304.
[37] B.J. Berne, M. Borkovec, J.E. Straub, Classical and modern methods in reaction-rate theory, J. Phys. Chem. 92 (1988) 3711–3725.
[38] M. Jacob, F.X. Schmid, Protein folding as a diffusional process, Biochemistry 38 (1999) 13773–13779.
[39] A.R. Fersht, A. Matouschek, L. Serrano, The folding of an enzyme. I. Theory of protein engineering analysis of stability and pathway of protein folding, J. Mol. Biol. 224 (1992) 771–782.
[40] A.N. Naganathan, U. Doshi, A. Fung, M. Sadqi, V. Muñoz, Dynamics, energetics, and structure in protein folding, Biochemistry 45 (2006) 8466–8475.
[41] F. Liu, M. Gruebele, Downhill dynamics and the molecular rate of protein folding, Chem. Phys. Lett. 461 (2008) 1–8.
[42] C.D. Snow, N. Nguyen, V.S. Pande, M. Gruebele, Absolute comparison of simulated and experimental protein-folding dynamics, Nature 420 (2002) 102–106.
[43] J. Kubelka, W.A. Eaton, J. Hofrichter, Experimental tests of villin subdomain folding simulations, J. Mol. Biol. 329 (2003) 625–630.
[44] D.M. Vu, E.S. Peterson, R.B. Dyer, Experimental resolution of early steps in protein folding: testing molecular dynamics simulations, J. Am. Chem. Soc. 126 (2004) 6546–6547.
[45] N.D. Socci, J.N. Onuchic, P.G. Wolynes, Diffusive dynamics of the reaction coordinate for protein folding funnels, J. Chem. Phys. 104 (1996) 5860–5868.
[46] E. Alm, D. Baker, Prediction of protein-folding mechanisms from free energy landscapes derived from native structures, Proc. Natl. Acad. Sci. USA 96 (1999) 11305–11310.
[47] O.V. Galzitskaya, A.V. Finkelstein, A theoretical search for folding/unfolding nuclei in three-dimensional protein structures, Proc. Natl. Acad. Sci. USA 96 (1999) 11299–11304.
[48] V. Muñoz, W.A. Eaton, A simple model for calculating the kinetics of protein folding from three-dimensional structures, Proc. Natl. Acad. Sci. USA 96 (1999) 11311–11316.
[49] M. Gruebele, Protein folding: the free energy surface, Curr. Opin. Struct. Biol. 12 (2002) 161–168.
[50] V. Muñoz, Conformational dynamics and ensembles in protein folding, Annu. Rev. Biophys. Biomol. Struct. 36 (2007) 395–412.
[51] R.B. Best, G. Hummer, Coordinate-dependent diffusion in protein folding, Proc. Natl. Acad. Sci. USA 107 (2010) 1088–1093.

[52] F. Noe, I. Horenko, C. Schutte, J.C. Smith, Hierarchical analysis of conformational dynamics in biomolecules transition networks of metastable states, J. Chem. Phys. 126 (2007) 155102.
[53] G.R. Bowman, X.H. Huang, V.S. Pande, Using generalized ensemble simulations and Markov state models to identify conformational states, Methods 49 (2009) 197–201.
[54] J.D. Chodera, N. Singhal, V.S. Pande, K.A. Dill, W.C. Swope, Automatic discovery of metastable states for the construction of Markov models of macromolecular conformational dynamics, J. Chem. Phys. 126 (2007) 155101.
[55] C.D. Snow, Y.M. Rhee, V.S. Pande, Kinetic definition of protein folding transition state ensembles and reaction coordinates, Biophys. J. 91 (2006) 14–24.
[56] S.P. Elmer, S. Park, V.S. Pande, Foldamer dynamics expressed via Markov state models. I. Explicit solvent molecular-dynamics simulations in acetonitrile, chloroform, methanol, and water, J. Chem. Phys. 123 (2005) 114902.
[57] S.P. Elmer, S. Park, V.S. Pande, Foldamer dynamics expressed via Markov state models. II. State space decomposition, J. Chem. Phys. 123 (2005) 114903.
[58] R.J. Wittebort, A. Szabo, Theory of NMR relaxation in macromolecules—restricted diffusion and jump models for multiple internal rotations in amino-acid side-chains, J. Chem. Phys. 69 (1978) 1722–1736.
[59] C.A. Royer, Probing protein folding and conformational transitions with fluorescence, Chem. Rev. 106 (2006) 1769–1784.
[60] S.E. Jackson, A.R. Fersht, Folding of chymotrypsin inhibitor-2.1. Evidence for a 2-state transition, Biochemistry 30 (1991) 10428–10435.
[61] M. Gruebele, The fast protein folding problem, Annu. Rev. Phys. Chem. 50 (1999) 485–516.
[62] B.E. Jones, J.M. Beechem, C.R. Matthews, Local and global dynamics during the folding of *Escherichia coli* dihydrofolate reductase by time-resolved fluorescence spectroscopy, Biochemistry 34 (1995) 1867–1877.
[63] M. Gruebele, J. Sabelko, R. Ballew, J. Ervin, Laser temperature jump induced protein refolding, Acc. Chem. Res. 31 (1998) 699–707.
[64] J. Ervin, J. Sabelko, M. Gruebele, Submicrosecond real-time fluorescence sampling: application to protein folding, J. Photochem. Photobiol. B 54 (2000) 1–15.
[65] P.A. Thompson, V. Muñoz, G.S. Jas, E.R. Henry, W.A. Eaton, J. Hofrichter, The helix-coil kinetics of a heteropeptide, J. Phys. Chem. B 104 (2000) 378–389.
[66] J. Kubelka, T.K. Chiu, D.R. Davies, W.A. Eaton, J. Hofrichter, Sub-microsecond protein folding, J. Mol. Biol. 359 (2006) 546–553.
[67] D.M. Vu, J.K. Myers, T.G. Oas, R.B. Dyer, Probing the folding and unfolding dynamics of secondary and tertiary structures in a three-helix bundle protein, Biochemistry 31 (2004) 3582–3589.
[68] D.J. Brockwell, D.A. Smith, S.E. Radford, Protein folding mechanisms: new methods and emerging ideas, Curr. Opin. Struct. Biol. 10 (2000) 16–25.
[69] K. Sridevi, G.S. Lakshmikanth, G. Krishnamoorthy, J.B. Udgaonkar, Increasing stability reduces conformational heterogeneity in a protein folding intermediate ensemble, J. Mol. Biol. 337 (2004) 699–711.
[70] E. Rhoades, E. Gussakovsky, G. Haran, Watching proteins fold one molecule at a time, Proc. Natl. Acad. Sci. USA 100 (2003) 3197–3202.
[71] B. Schuler, Single-molecule fluorescence spectroscopy of protein folding, Chemphyschem 6 (2005) 1206–1220.
[72] K.M. Hamadani, S. Weiss, Nonequilibrium single molecule protein folding in a coaxial mixer, Biophys. J. 95 (2008) 352–365.
[73] B. Schuler, E.A. Lipman, W.A. Eaton, Probing the free-energy surface for protein folding with single-molecule fluorescence spectroscopy, Nature 419 (2002) 743–747.
[74] A. Barth, C. Zscherp, What vibrations tell us about proteins, Q. Rev. Biophys. 35 (2002) 369–430.
[75] S.M. Decatur, Elucidation of residue-level structure and dynamics of polypeptides via isotope-edited infrared spectroscopy, Acc. Chem. Res. 39 (2006) 169–175.
[76] K.E. Amunson, L. Ackels, J. Kubelka, Site-specific unfolding thermodynamics of a helix-turn-helix protein, J. Am. Chem. Soc. 130 (2008) 8146–8147.
[77] S.T.R. Walsh, R.P. Cheng, W.W. Wright, D.O.V. Alonso, V. Daggett, J.M. Vanderkooi, W.F. DeGrado, The hydration of amides in helices; a comprehensive picture from molecular dynamics, IR, and NMR, Protein Sci. 12 (2003) 520–531.
[78] S.H. Brewer, B.B. Song, D.P. Raleigh, R.B. Dyer, Residue specific resolution of protein folding dynamics using isotope-edited infrared temperature jump spectroscopy, Biochemistry 46 (2007) 3279–3285.
[79] K. Gerwert, Molecular reaction mechanisms of proteins as monitored by time-resolved FTIR spectroscopy, Curr. Opin. Struct. Biol. 3 (1993) 769–773.
[80] P. Lia, F.Y. Oliva, A.N. Naganathan, V. Muñoz, Dynamics of one-state downhill protein folding, Proc. Natl. Acad. Sci. USA 106 (2009) 103–108.
[81] R.B. Dyer, F. Gai, W.H. Woodruff, Infrared studies of fast events in protein folding, Acc. Chem. Res. 31 (1998) 709–716.
[82] H.R. Ma, J. Ervin, M. Gruebele, Single-sweep detection of relaxation kinetics by submicrosecond midinfrared spectroscopy, Rev. Sci. Instrum. 75 (2004) 486–491.
[83] J. Bredenbeck, J. Helbing, P. Hamm, Continuous scanning from picoseconds to microseconds in time resolved linear and nonlinear spectroscopy, Rev. Sci. Instrum. 75 (2004) 4462–4466.
[84] J. Wang, M.A. El-Sayed, Temperature jump-induced secondary structural change of the membrane protein bacteriorhodopsin in the premelting temperature region: a nanosecond time-resolved Fourier transform infrared study, Biophys. J. 76 (1999) 2777–2783.
[85] P. Hamm, J. Helbing, J. Bredenbeck, Two-dimensional infrared spectroscopy of photoswitchable peptides, Annu. Rev. Phys. Chem. 59 (2008) 291–317.
[86] H.S. Chung, M. Khalil, A. Tokmakoff, Nonlinear infrared spectroscopy of protein conformational change during thermal unfolding, J. Phys. Chem. B 108 (2004) 15332–15342.
[87] G. Balakrishnan, Y. Hu, G.M. Bender, Z. Getahun, W.F. DeGrado, T.G. Spiro, Enthalpic and entropic stages in alpha-helical peptide unfolding, from laser T-Jump/UV raman spectroscopy, J. Am. Chem. Soc. 129 (2007) 12801–12808.
[88] A.V. Mikhonin, S.V. Bykov, N.S. Myshakina, S.A. Asher, Peptide secondary structure folding reaction coordinate: correlation between UV Raman amide III frequency, Psi Ramachandran angle, and hydrogen bonding, J. Phys. Chem. B 110 (2006) 1928–1943.
[89] T. Jordan, T.G. Spiro, Enhancement of C-alpha hydrogen vibrations in the resonance Raman spectra of amides, J. Raman Spectrosc. 25 (1994) 537–543.
[90] A. Ianoul, A. Mikhonin, I.K. Lednev, S.A. Asher, UV resonance Raman study of the spatial dependence of alpha-helix unfolding, J. Phys. Chem. A 106 (2002) 3621–3624.
[91] E.F. Chen, P. Wittung-Stafshede, D.S. Kliger, Far-UV time-resolved circular dichroism detection of electron-transfer-triggered cytochrome *c* folding, J. Am. Chem. Soc. 121 (1999) 3811–3817.
[92] E.F. Chen, Y.X. Wen, J.W. Lewis, R.A. Goldbeck, D.S. Kliger, C.E.M. Strauss, Nanosecond laser temperature-jump optical rotatory dispersion: application to early events in protein folding/unfolding, Rev. Sci. Instrum. 76 (2005).
[93] E. Chen, R.A. Goldbeck, D.S. Kliger, Probing early events in ferrous cytochrome *c* folding with time-resolved natural and magnetic circular dichroism spectroscopies, Curr. Prot. Pept. Sci. 10 (2009) 464–475.
[94] T.K.S. Kumar, C. Yu, Monitoring protein folding at atomic resolution, Acc. Chem. Res. 37 (2004) 929–936.
[95] H.J. Dyson, P.E. Wright, Insights into protein folding from NMR, Annu. Rev. Phys. Chem. 47 (1996) 369–395.
[96] D.F. Hansen, H.Q. Feng, Z. Zhou, Y.W. Bai, L.E. Kay, Selective characterization of microsecond motions in proteins by NMR relaxation, J. Am. Chem. Soc. 131 (2009) 16257–16265.
[97] A. Mittermaier, L.E. Kay, New tools provide new insights in NMR studies of protein dynamics, Science 312 (2006) 224–228.
[98] A.G. Palmer III, NMR characterization of the dynamics of biomacromolecules, Chem. Rev. 104 (2004) 3623–3640.
[99] S. Schwarzinger, R. Mohana-Borges, G.J.A. Kroon, H.J. Dyson, P.E. Wright, Structural characterization of partially folded intermediates of apomyoglobin H64F, Protein Sci. 17 (2008) 313–321.
[100] D.J. Felitsky, M.A. Lietzow, H.J. Dyson, P.E. Wright, Modeling transient collapsed states of an unfolded protein to provide insights into early folding events, Proc. Natl. Acad. Sci. USA 105 (2008) 6278–6283.
[101] S.W. Englander, Protein folding intermediates and pathways studied by hydrogen exchange, Annu. Rev. Biophys. Biomol. Struct. 29 (2000) 213–238.
[102] S.W. Englander, L. Mayne, M.M.G. Krishna, Protein folding and misfolding: mechanism and principles, Q. Rev. Biophys. 40 (2007) 287–326.
[103] L. Konermann, X. Tong, Y. Pan, Protein structure and dynamics studied by mass spectrometry: H/D exchange, hydroxyl radical labeling, and related approaches, J. Mass Spectrom. 43 (2008) 1021–1036.
[104] S. Akiyama, S. Takahashi, T. Kimura, K. Ishimori, I. Morishima, Y. Nishikawa, T. Fujisawa, Conformational landscape of cytochrome *c* folding studied by microsecond-resolved small-angle x-ray scattering, Proc. Natl. Acad. Sci. USA 99 (2002) 1329–1334.
[105] R.P. Rambo, J.A. Tainer, Bridging the solution divide: comprehensive structural analyses of dynamic RNA, DNA, and protein assemblies by small-angle X-ray scattering, Curr. Opin. Struct. Biol. 20 (2010) 128-137.
[106] I.S. Millet, L.E. Townsley, F. Chiti, S. Doniach, K.W. Plaxco, Equilibrium collapse and the kinetic 'foldability' of proteins, Biochemistry 41 (2002) 321–325.
[107] J. Lipfert, S. Doniach, Small-angle X-ray scattering from RNA, proteins, and protein complexes, Annu. Rev. Biophys. Biomol. Struct. 36 (2007) 307–327.
[108] K.C. Hansen, R.S. Rock, R.W. Larsen, S.I. Chan, A method for photoinitating protein folding in a nondenaturing environment, J. Am. Chem. Soc. 122 (2000) 11567–11568.
[109] V.M. Grigoryants, A.V. Veselov, C.P. Scholes, Variable velocity liquid flow EPR applied to submillisecond protein folding, Biophys. J. 78 (2000) 2702–2708.
[110] V. Belle, S. Rouger, S. Costanzo, E. Liquiere, J. Strancar, B. Guigliarelli, A. Fournel, S. Longhi, Mapping alpha-helical induced folding within the intrinsically disordered C-terminal domain of the measles virus nucleoprotein by site-directed spin-labeling EPR spectroscopy, Proteins Struct. Funct. Bioinform. 73 (2008) 973–988.
[111] T. Kiefhaber, F.X. Schmid, K. Willaert, Y. Engelborghs, A. Chaffotte, Structure of a rapidly formed intermediate in ribonuclease-T1 folding, Protein Sci. 1 (1992) 1162–1172.
[112] T.Y. Tsong, Ferricytochrome *c* chain folding measured by the energy transfer of tryptophan 59 to the heme group, Biochemistry 15 (1976) 5467–5473.
[113] C. Tanford, K.C. Aune, A. Ikai, Kinetics of unfolding and refolding of proteins. 3. Results for lysozyme, J. Mol. Biol. 73 (1973) 185–197.
[114] H. Roder, W. Colon, Kinetic role of early intermediates in protein folding, Curr. Opin. Struct. Biol. 7 (1997) 15–28.
[115] P. Regenfuss, R.M. Clegg, M.J. Fulwyler, F.J. Barrantes, T.M. Jovin, Mixing liquids in microseconds, Rev. Sci. Instrum. 56 (1985) 283–290.
[116] H. Roder, K. Maki, H. Cheng, M.C.R. Shastry, Rapid mixing methods for exploring the kinetics of protein folding, Methods 34 (2004) 15–27.
[117] I. Grillo, Applications of stopped-flow in SAXS and SANS, Curr. Opin. Colloid Interface Sci. 14 (2009) 402–408.
[118] H. Roder, K. Maki, H. Cheng, Early events in protein folding explored by rapid mixing methods, Chem. Rev. 106 (2006) 1836–1861.
[119] L.J. Lapidus, S.H. Yao, K.S. McGarrity, D.E. Hertzog, E. Tubman, O. Bakajin, Protein hydrophobic collapse and early folding steps observed in a microfluidic mixer, Biophys. J. 93 (2007) 218–224.

[120] S.A. Waldauer, O. Bakajin, T. Ball, Y. Chen, S.J. DeCamp, M. Kopka, M. Jager, V.R. Singh, W.J. Wedemeyer, S. Weiss, S. Yao, L.J. Lapidus, Ruggedness in the folding landscape of protein L, HFSP J. 2 (2008) 388–395.
[121] A.S. Kane, A. Hoffmann, P. Baumgartel, R. Seckler, G. Reichardt, D.A. Horsley, B. Schuler, O. Bakajin, Microfluidic mixers for the investigation of rapid protein folding kinetics using synchrotron radiation circular dichroism spectroscopy, Anal. Chem. 80 (2008) 9534–9541.
[122] E.A. Lipman, B. Schuler, O. Bakajin, W.A. Eaton, Single-molecule measurement of protein folding kinetics, Science 301 (2003) 1233–1235.
[123] S.H. Pfeil, C.E. Wickersham, A. Hoffmann, E.A. Lipman, A microfluidic mixing system for single-molecule measurements, Rev. Sci. Instrum. 80 (2009).
[124] R.B. Dyer, F. Gai, W.H. Woodruff, Infrared studies of fast events in protein folding, Acc. Chem. Res. 31 (1998) 709–716.
[125] B. Nolting, R. Golbik, A.R. Fersht, Submillisecond events in protein folding, Proc. Natl. Acad. Sci. USA 92 (1995) 10668–10672.
[126] C.A. Royer, Revisiting volume changes in pressure-induced protein unfolding, BBA-Protein Struct. Mol. Enzym. 1595 (2002) 201–209.
[127] F. Meersman, C.M. Dobson, K. Heremans, Protein unfolding, amyloid fibril formation and configurational energy landscapes under high pressure conditions, Chem. Soc. Rev. 35 (2006) 908–917.
[128] M. Eigen, L. de Mayer, Relaxation methods, in: A. Weisberger (Ed.), Techniques in Organic Chemistry, Part II, Wiley: Interscience, New York, 1963, pp. 895–1054.
[129] B. Nolting, Protein Folding Kinetics. Biophysical Methods, 2nd ed. Springer, Berlin, 2006.
[130] J. Kubelka, Time-resolved methods in biophysics. 9. Laser temperature-jump methods for investigating biomolecular dynamics, Photochem. Photobiol. Sci. 8 (2009) 499–512.
[131] J.V. Beitz, G.W. Flynn, D.H. Turner, N. Sutin, Stimulated Raman effect—a new source of laser temperature-jump heating, J. Am. Chem. Soc. 92 (1970) 4130–4132.
[132] S. Ameen, Laser temperature-jump spectrophotometer using stimulated Raman effect in H_2 gas for study of nanosecond fast chemical relaxation times, Rev. Sci. Instrum. 46 (1975) 1209–1215.
[133] S. Williams, T.P. Causgrove, R. Gilmanshin, K.S. Fang, R.H. Callender, W.H. Woodruff, R.B. Dyer, Fast events in protein folding. Helix melting and formation in a small peptide, Biochemistry 35 (1996) 691–697.
[134] G. Balakrishnan, Y. Hu, M.A. Case, T.G. Spiro, Microsecond melting of a folding intermediate in a coiled-coil peptide, monitored by T-jump/UV Raman spectroscopy, J. Phys. Chem. B 110 (2006) 19877–19883.
[135] M. Sadqi, L.J. Lapidus, V. Muñoz, How fast is protein hydrophobic collapse? Proc. Natl. Acad. Sci. USA 100 (2003) 12117–12122.
[136] R.M. Clegg, B.W. Maxfield, Chemical kinetic studies by a new small pressure perturbation method, Rev. Sci. Instrum. 47 (1976) 1383–1393.
[137] M. Oliveberg, A.R. Fersht, Thermodynamics of transient conformations in the folding pathway of barnase—reorganization of the folding intermediate at low pH, Biochemistry 35 (1996) 2738–2749.
[138] M. Jacob, G. Holtermann, D. Perl, J. Reinstein, T. Schindler, M.A. Geeves, F.X. Schmid, Microsecond folding of the cold shock protein measured by a pressure-jump technique, Biochemistry 38 (1999) 2882–2891.
[139] C.M. Jones, E.R. Henry, Y. Hu, C.K. Chan, S.D. Luc, A. Bhuyan, H. Roder, J. Hofrichter, W.A. Eaton, Fast events in protein folding initiated by nanosecond laser photolysis, Proc. Natl. Acad. Sci. USA 90 (1993) 11860–11864.
[140] T. Pascher, J.P. Chesick, J.R. Winkler, H.B. Gray, Protein folding triggered by electron transfer, Science 271 (1996) 1558–1560.
[141] J. Bredenbeck, J. Helbing, J.R. Kumita, G.A. Woolley, P. Hamm, alpha-helix formation in a photoswitchable peptide tracked from picoseconds to microseconds by time-resolved IR spectroscopy, Proc. Natl. Acad. Sci. USA 102 (2005) 2379–2384.
[142] R.S. Rock, K.C. Hansen, R.W. Larsen, S.I. Chan, Rapid photochemical triggering of protein unfolding in a nondenaturing environment, Chem. Phys. 307 (2004) 201–208.
[143] M. Volk, Fast initiation of peptide and protein folding processes, Eur. J. Org. Chem. (2001) 2605–2621.
[144] H.S.M. Lu, M. Volk, Y. Kholodenko, E. Gooding, R.M. Hochstrasser, W.F. DeGrado, Aminothiotyrosine disulfide, an optical trigger for initiation of protein folding, J. Am. Chem. Soc. 119 (1997) 7173–7180.
[145] S.L. Dong, M. Loweneck, T.E. Schrader, W.J. Schreier, W. Zinth, L. Moroder, C. Renner, A photocontrolled beta-hairpin peptide, Chem. Eur. J. 12 (2006) 1114–1120.
[146] J.R. Forman, J. Clarke, Mechanical unfolding of proteins: insights into biology, structure and folding, Curr. Opin. Struct. Biol. 17 (2007) 58–66.
[147] M. Rief, M. Gautel, F. Oesterhelt, J.M. Fernandez, H.E. Gaub, Reversible unfolding of individual titin immunoglobulin domains by AFM, Science 276 (1997) 1109–1112.
[148] M.S.Z. Kellermayer, S.B. Smith, H.L. Granzier, C. Bustamante, Folding–unfolding transitions in single titin molecules characterized with laser tweezers, Science 276 (1997) 1112–1116.
[149] C. Cecconi, E.A. Shank, C. Bustamante, S. Marqusee, Direct observation of the three-state folding of a single protein molecule, Science 309 (2005) 2057–2060.
[150] M. Schlierf, H.B. Li, J.M. Fernandez, The unfolding kinetics of ubiquitin captured with single-molecule force-clamp techniques, Proc. Natl. Acad. Sci. USA 101 (2004) 7299–7304.
[151] J.M. Fernandez, H.B. Li, Force-clamp spectroscopy monitors the folding trajectory of a single protein, Science 303 (2004) 1674–1678.
[152] S. Garcia-Manyes, L. Dougan, C.L. Badilla, J. Brujic, J.M. Fernandez, Direct observation of an ensemble of stable collapsed states in the mechanical folding of ubiquitin, Proc. Natl. Acad. Sci. USA 106 (2009) 10534–10539.
[153] J.K. Myers, T.G. Oas, Mechanisms of fast protein folding, Annu. Rev. Biochem. 71 (2002) 783–815.
[154] G.S. Huang, T.G. Oas, Submillisecond folding of monomeric lambda-repressor, Proc. Natl. Acad. Sci. USA 92 (1995) 6878–6882.
[155] J.K. Myers, T.G. Oas, Preorganized secondary structure as an important determinant of fast protein folding, Nat. Struct. Biol. 8 (2001) 552–558.
[156] M.H. Wang, Y.F. Tang, S.S. Sato, L. Vugmeyster, C.J. McKnight, D.P. Raleigh, Dynamic NMR line-shape analysis demonstrates that the villin headpiece subdomain folds on the microsecond time scale, J. Am. Chem. Soc. 125 (2003) 6032–6033.
[157] P. Neudecker, P. Lundstrom, L.E. Kay, Relaxation dispersion NMR spectroscopy as a tool for detailed studies of protein folding, Biophys. J. 96 (2009) 2045–2054.
[158] B. Gillespie, D.M. Vu, P.S. Shah, S.A. Marshall, R.B. Dyer, S.L. Mayo, K.W. Plaxco, NMR and temperature-jump measurements of de novo designed proteins demonstrate rapid folding in the absence of explicit selection for kinetics, J. Mol. Biol. 330 (2003) 813–819.
[159] D.M. Korzhnev, X. Salvatella, M. Vendruscolo, A.A. Di Nardo, A.R. Davidson, C.M. Dobson, L.E. Kay, Low-populated folding intermediates of Fyn SH3 characterized by relaxation dispersion NMR, Nature 430 (2004) 586–590.
[160] E.V. Kuzmenkina, C.D. Heyes, G.U. Nienhaus, Single-molecule Forster resonance energy transfer study of protein dynamics under denaturing conditions, Proc. Natl. Acad. Sci. USA 102 (2005) 15471–15476.
[161] H.S. Chung, J.M. Louis, W.A. Eaton, Experimental determination of upper bound for transition path times in protein folding from single-molecule photon-by-photon trajectories, Proc. Natl. Acad. Sci. USA 106 (2009) 11837–11844.
[162] F. Huang, S. Sato, T.D. Sharpe, L.M. Ying, A.R. Fersht, Distinguishing between cooperative and unimodal downhill protein folding, Proc. Natl. Acad. Sci. USA 104 (2007) 123–127.
[163] S.T. Hess, S.H. Huang, A.A. Heikal, W.W. Webb, Biological and chemical applications of fluorescence correlation spectroscopy: a review, Biochemistry 41 (2002) 697–705.
[164] E. Haustein, P. Schwille, Fluorescence correlation spectroscopy: novel variations of an established technique, Annu. Rev. Biophys. Biomol. Struct. 36 (2007) 151–169.
[165] H. Neuweiler, S. Doose, M. Sauer, A microscopic view of miniprotein folding: enhanced folding efficiency through formation of an intermediate, Proc. Natl. Acad. Sci. USA 102 (2005) 16650–16655.
[166] K. Chattopadhyay, E.L. Elson, C. Frieden, The kinetics of conformational fluctuations in an unfolded protein measured by fluorescence methods, Proc. Natl. Acad. Sci. USA 102 (2005) 2385–2389.
[167] H. Neuweiler, C.M. Johnson, A.R. Fersht, Direct observation of ultrafast folding and denatured state dynamics in single protein molecules, Proc. Natl. Acad. Sci. USA 106 (2009) 18569–18574.
[168] N. Ferguson, A.R. Fersht, Early events in protein folding, Curr. Opin. Struct. Biol. 13 (2003) 75–81.
[169] G. Schwarz, On kinetics of helix-coil transition of polypeptides in solution, J. Mol. Biol. 11 (1965) 64–77.
[170] G.G. Hammes, P.B. Roberts, Dynamics of helix-coil transition in poly-L-ornithine, J. Am. Chem. Soc. 91 (1969) 1812–1816.
[171] S. Marqusee, V.H. Robbins, R.L. Baldwin, Unusually stable helix formation in short alanine-based peptides, Proc. Natl. Acad. Sci. USA 86 (1989) 5286–5290.
[172] I.K. Lednev, A.S. Karnoup, M.C. Sparrow, S.A. Asher, Alpha-helix peptide folding and unfolding activation barriers: a nanosecond UV resonance raman study, J. Am. Chem. Soc. 121 (1999) 8074–8086.
[173] C.Y. Huang, Z. Getahun, Y.J. Zhu, J.W. Klemke, W.F. DeGrado, F. Gai, Helix formation via conformation diffusion search, Proc. Natl. Acad. Sci. USA 99 (2002) 2788–2793.
[174] J.A. Ihalainen, B. Paoli, S. Muff, E.H.G. Backus, J. Bredenbeck, G.A. Woolley, A. Caflisch, P. Hamm, Alpha-helix folding in the presence of structural constraints, Proc. Natl. Acad. Sci. USA 105 (2008) 9588–9593.
[175] J.A. Ihalainen, J. Bredenbeck, R. Pfister, J. Helbing, L. Chi, I.H.M. van Stokkum, G.A. Woolley, P. Hamm, Folding and unfolding of a photoswitchable peptide from picoseconds to microseconds, Proc. Natl. Acad. Sci. USA 104 (2007) 5383–5388.
[176] C.Y. Huang, Z. Getahun, T. Wang, W.F. DeGrado, F. Gai, Time-resolved infrared study of the helix-coil transition using C-13-labeled helical peptides, J. Am. Chem. Soc. 123 (2001) 12111–12112.
[177] A.P. Ramajo, S.A. Petty, A. Starzyk, S.M. Decatur, M. Volk, The alpha-helix folds more rapidly at the C-terminus than at the N-terminus, J. Am. Chem. Soc. 127 (2005) 13784–13785.
[178] A.V. Mikhonin, S.A. Asher, S.V. Bykov, A. Murza, UV Raman spatially resolved melting dynamics of isotopically labeled polyalanyl peptide: slow alpha-helix melting follows 3(10)-helices and pi-bulges premelting, J. Phys. Chem. B 111 (2007) 3280–3292.
[179] U.R. Doshi, V. Muñoz, The principles of alpha-helix formation: explaining complex kinetics with nucleation-elongation theory, J. Phys. Chem. B 108 (2004) 8497–8506.
[180] S. Mukherjee, P. Chowdhury, M.R. Bunagan, F. Gai, Folding kinetics of a naturally occurring helical peptide: implication of the folding speed limit of helical proteins, J. Phys. Chem. B 112 (2008) 9146–9150.
[181] S.A. Petty, M. Volk, Fast folding dynamics of an alpha-helical peptide with bulky side chains, Phys. Chem. Chem. Phys. 6 (2004) 1022–1030.
[182] R. Gilmanshin, S. Williams, R.H. Callender, W.H. Woodruff, R.B. Dyer, Fast events in protein folding—relaxation dynamics of secondary and tertiary structure in native apomyoglobin, Proc. Natl. Acad. Sci. USA 94 (1997) 3709–3713.
[183] F.J. Blanco, G. Rivas, L. Serrano, A short peptide that folds into a native stable beta-hairpin in aqueous solution, Nat. Struct. Biol. 1 (1994) 584–590.
[184] V. Muñoz, P.A. Thompson, J. Hofrichter, Folding dynamics and mechanism of beta-hairpin formation, Nature 390 (1997) 196–199.

[185] V. Muñoz, E.R. Henry, J. Hofrichter, W.A. Eaton, A statistical mechanical model for beta-hairpin kinetics, Proc. Natl. Acad. Sci. USA 95 (1998) 5872–5879.
[186] E.R. Henry, V. Muñoz, W.A. Eaton, Combinatorial modeling of protein folding kinetics, Biophys. J. 82 (2002) 1466.
[187] V.S. Pande, D.S. Rokhsar, Molecular dynamics simulations of unfolding and refolding of a beta-hairpin fragment of protein G, Proc. Natl. Acad. Sci. USA 96 (1999) 9062–9067.
[188] A.R. Dinner, T. Lazaridis, M. Karplus, Understanding β-hairpin formation, Proc. Natl. Acad. Sci. USA 96 (1999) 9068–9073.
[189] D.K. Klimov, D. Thirumalai, Mechanisms and kinetics of beta-hairpin formation, Proc. Natl. Acad. Sci. USA 97 (2000) 2544–2549.
[190] A.E. Garcia, K.Y. Sanbonmatsu, Exploring the energy landscape of a beta hairpin in explicit solvent, Proteins Struct. Funct. Gen. 42 (2001) 345–354.
[191] H.W. Wu, S.M. Wang, B.R. Brooks, Direct observation of the folding and unfolding of a beta- hairpin in explicit water through computer simulation, J. Am. Chem. Soc. 124 (2002) 5282–5283.
[192] G.H. Wei, P. Derreumaux, N. Mousseau, Sampling the complex energy landscape of a simple beta-hairpin, J. Chem. Phys. 119 (2003) 6403–6406.
[193] P.G. Bolhuis, Transition-path sampling of beta-hairpin folding, Proc. Natl. Acad. Sci. USA 100 (2003) 12129–12134.
[194] C.D. Snow, L.L. Qiu, D.G. Du, F. Gai, S.J. Hagen, V.S. Pande, Trp zipper folding kinetics by molecular dynamics and temperature-jump spectroscopy, Proc. Natl. Acad. Sci. USA 101 (2004) 4077–4082.
[195] D.G. Du, Y.J. Zhu, C.Y. Huang, F. Gai, Understanding the key factors that control the rate of beta-hairpin folding, Proc. Natl. Acad. Sci. USA 101 (2004) 15915–15920.
[196] W.Y. Yang, M. Gruebele, Detection-dependent kinetics as a probe of folding landscape microstructure, J. Am. Chem. Soc. 126 (2004) 7758–7759.
[197] D.G. Du, F. Gai, Understanding the folding mechanism of an alpha-helical hairpin, Biochemistry 45 (2006) 13131–13139.
[198] Y. Xu, P. Purkayastha, F. Gai, Nanosecond folding dynamics of a three-stranded beta-sheet, J. Am. Chem. Soc. 128 (2006) 15836–15842.
[199] Y. Xu, M.R. Bunagan, J. Tang, F. Gai, Probing the kinetic cooperativity of beta-sheet folding perpendicular to the strand direction, Biochemistry 47 (2008) 2064–2070.
[200] F. Huang, W.M. Nau, A conformational flexibility scale for amino acids in peptides, Angew. Chem. Int. Ed. 42 (2003) 2269–2272.
[201] A. Moglich, K. Joder, T. Kiefhaber, End-to-end distance distributions and intrachain diffusion constants in unfolded polypeptide chains indicate intramolecular hydrogen bond formation, Proc. Natl. Acad. Sci. USA 103 (2006) 12394–12399.
[202] O. Bieri, J. Wirz, B. Hellrung, M. Schutlowski, M. Drewello, T. Kiefhaber, The speed limit for protein folding measured by triplet-triplet energy transfer, Proc. Natl. Acad. Sci. USA 96 (1999).
[203] L.J. Lapidus, W.A. Eaton, J. Hofrichter, Measuringthe rate of intramolecular contact formation in polypeptides, Proc. Natl. Acad. Sci. USA 97 (2000) 7220–7225.
[204] M. Buscaglia, L.J. Lapidus, W.A. Eaton, J. Hofrichter, Effects of denaturants on the dynamics of loop formation in polypeptides, Biophys. J. 91 (2006) 276–288.
[205] F. Krieger, B. Fierz, O. Bieri, M. Drewello, T. Kiefhaber, Dynamics of unfolded polypeptide chains as model for the earliest steps in protein folding, J. Mol. Biol. 332 (2003) 265–274.
[206] A. Szabo, K. Schulten, Z. Schulten, 1st passage time approach to diffusion controlled reactions, J. Chem. Phys. 72 (1980) 4350–4357.
[207] B. Fierz, T. Kiefhaber, End-to-end vs interior loop formation kinetics in unfolded polypeptide chains, J. Am. Chem. Soc. 129 (2007) 672–679.
[208] A. Soranno, R. Longhi, T. Bellini, M. Buscaglia, Kinetics of contact formation and end-to-end distance distributions of swollen disordered peptides, Biophys. J. 96 (2009) 1515–1528.
[209] I.V. Gopich, D. Nettels, B. Schuler, A. Szabo, Protein dynamics from single-molecule fluorescence intensity correlation functions, J. Chem. Phys. 131 (2009).
[210] D. Nettels, A. Hoffmann, B. Schuler, Unfolded protein and peptide dynamics investigated with single-molecule FRET and correlation spectroscopy from picoseconds to seconds, J. Phys. Chem. B 112 (2008) 6137–6146.
[211] A. Hoffmann, A. Kane, D. Nettels, D.E. Hertzog, P. Baumgartel, J. Lengefeld, G. Reichardt, D.A. Horsley, R. Seckler, O. Bakajin, B. Schuler, Mapping protein collapse with single-molecule fluorescence and kinetic synchrotron radiation circular dichroism spectroscopy, Proc. Natl. Acad. Sci. USA 104 (2007) 105–110.
[212] I.V. Gopich, A. Szabo, Single-macromolecule fluorescence resonance energy transfer and free-energy profiles, J. Phys. Chem. B 107 (2003) 5058–5063.
[213] G. Ziv, D. Thirumalai, G. Haran, Collapse transition in proteins, Phys. Chem. Chem. Phys. 11 (2009) 83–93.
[214] K.W. Plaxco, I.S. Millett, D.J. Segel, S. Doniach, D. Baker, Chain collapse can occur concomitantly with the rate-limiting step in protein folding, Nat. Struct. Biol. 6 (1999) 554–556.
[215] C.J. Camacho, D. Thirumalai, Kinetics and thermodynamics of folding in model proteins, Proc. Natl. Acad. Sci. USA 90 (1993) 6369–6372.
[216] C. Magg, J. Kubelka, G. Holtermann, E. Haas, F.X. Schmid, Specificity of the initial collapse in the folding of the cold shock protein, J. Mol. Biol. 360 (2006) 1067–1080.
[217] S.J. Hagen, W.A. Eaton, Two-state expansion and collapse of a polypeptide, J. Mol. Biol. 301 (2000) 1019–1027.
[218] E. Sherman, G. Haran, Coil-globule transition in the denatured state of a small protein, Proc. Natl. Acad. Sci. USA 103 (2006) 11539–11543.
[219] L. Pollack, M.W. Tate, N.C. Darnton, J.B. Knight, S.M. Gruner, W.A. Eaton, R.H. Austin, Compactness of the denatured state of a fast-folding protein measured by submillisecond small-angle x-ray scattering, Proc. Natl. Acad. Sci. USA 96 (1999) 10115–10117.
[220] R.B. Dyer, Ultrafast and downhill protein folding, Curr. Opin. Struct. Biol. 17 (2007) 38–47.
[221] N. Ferguson, C.M. Johnson, M. Macias, H. Oschkinat, A. Fersht, Ultrafast folding of WW domains without structured aromatic clusters in the denatured state, Proc. Natl. Acad. Sci. USA 98 (2001) 13002–13007.
[222] H. Nguyen, M. Jager, A. Moretto, M. Gruebele, J.W. Kelly, Tuning the free-energy landscape of a WW domain by temperature, mutation, and truncation, Proc. Natl. Acad. Sci. USA 100 (2003) 3948–3953.
[223] A. Fung, P. Li, R. Godoy-Ruiz, J.M. Sanchez-Ruiz, V. Muñoz, Expanding the realm of ultrafast protein folding: gpW, a midsize natural single-domain with alpha +beta topology that folds downhill, J. Am. Chem. Soc. 130 (2008) 7489–7495.
[224] U. Mayor, N.R. Guydosh, C.M. Johnson, J.G. Grossmann, S. Sato, G.S. Jas, S.M.V. Freund, D.O.V. Alonso, V. Daggett, A.R. Fersht, The complete folding pathway of a protein from nanoseconds to microseconds, Nature 421 (2003) 863–867.
[225] W.Y. Yang, M. Gruebele, Folding at the speed limit, Nature 423 (2003) 193–197.
[226] T.L. Religa, C.M. Johnson, D.M. Vu, S.H. Brewer, R.B. Dyer, A.R. Fersht, The helix-turn-helix motif as an ultrafast independently folding domain: the pathways of folding of Engrailed homeodomain, Proc. Natl. Acad. Sci. USA 104 (2007) 9272–9277.
[227] S. Sato, T.L. Religa, V. Daggett, A.R. Fersht, Testing protein folding simulations by experiment: B domain of protein A, Proc. Natl. Acad. Sci. USA 101 (2004) 6952–6956.
[228] S.H. Brewer, D.M. Vu, Y.F. Tang, Y. Li, S. Franzen, D.P. Raleigh, R.B. Dyer, Effect of modulating unfolded state structure on the folding kinetics of the villin headpiece subdomain, Proc. Natl. Acad. Sci. USA 102 (2005) 16662–16667.
[229] Y.F. Tang, M.J. Goger, D.P. Raleigh, NMR characterization of a peptide model provides evidence for significant structure in the unfolded state of the villin headpiece helical subdomain, Biochemistry 45 (2006) 6940–6946.
[230] J. Kubelka, E.R. Henry, T. Cellmer, J. Hofrichter, W.A. Eaton, Chemical, physical, and theoretical kinetics of an ultrafast folding protein, Proc. Natl. Acad. Sci. USA 105 (2008) 18655–18662.
[231] H.X. Lei, Y. Duan, Two-stage folding of HP-35 from ab initio simulations, J. Mol. Biol. 370 (2007) 196–206.
[232] A. Reiner, P. Henklein, T. Kiefhaber, An unlocking/relocking barrier in conformational fluctuations of villin headpiece subdomain, Proc. Natl. Acad. Sci. USA 107 (2010) 4955–4960.
[233] W.Y. Yang, M. Gruebele, Rate-temperature relationships in lambda-repressor fragment lambda(6-85) folding, Biochemistry 43 (2004) 13018–13025.
[234] H.R. Ma, M. Gruebele, Kinetics are probe-dependent during downhill folding of an engineered lambda(6-85) protein, Proc. Natl. Acad. Sci. USA 102 (2005) 2283–2287.
[235] F. Liu, M. Nakaema, M. Gruebele, The transition state transit time of WW domain folding is controlled by energy landscape roughness, J. Chem. Phys. 131 (2009).
[236] W.Y. Yang, M. Gruebele, Folding lambda repressor at its speed limit, Biophys. J. 87 (2004) 596–608.
[237] H.R. Ma, M. Gruebele, Low barrier kinetics: dependence on observables and free energy surface, J. Comput. Chem. 27 (2006) 125–134.
[238] S.J. Hagen, Probe-dependent and nonexponential relaxation kinetics: unreliable signatures of downhill protein folding, Proteins-Struct. Funct. Bioinform. 68 (2007) 205–217.
[239] M. Knott, H.S. Chan, Criteria for downhill protein folding: calorimetry, chevron plot, kinetic relaxation, and single-molecule radius of gyration in chain models with subdued degrees of cooperativity, Proteins-Struct. Funct. Bioinform. 65 (2006) 373–391.
[240] F. Liu, M. Gruebele, Tuning lambda(6-85) towards downhill folding at its melting temperature, J. Mol. Biol. 370 (2007) 574–584.
[241] V. Muñoz, Thermodynamics and kinetics of downhill protein folding investigated with a simple statistical mechanical model, Int. J. Quantum Chem. 90 (2002) 1522–1528.
[242] F.Y. Oliva, V. Muñoz, A simple thermodynamic test to discriminate between two-state and downhill folding, J. Am. Chem. Soc. 126 (2004) 8596–8597.
[243] M.M. Garcia-Mira, M. Sadqi, N. Fischer, J.M. Sanchez-Ruiz, V. Muñoz, Experimental identification of downhill protein folding, Science 298 (2002) 2191–2195.
[244] M. Sadqi, D. Fushman, V. Muñoz, Atom-by-atom analysis of global downhill protein folding, Nature 442 (2006) 317–321.
[245] V. Muñoz, J.M. Sanchez-Ruiz, Exploring protein-folding ensembles: a variable-barrier model for the analysis of equilibrium unfolding experiments, Proc. Natl. Acad. Sci. USA 101 (2004) 17646–17651.
[246] A.N. Naganathan, J.M. Sanchez-Ruiz, V. Muñoz, Direct measurement of barrier heights in protein folding, J. Am. Chem. Soc. 127 (2005) 17970–17971.
[247] R. Godoy-Ruiz, E.R. Henry, J. Kubelka, J. Hofrichter, V. Muñoz, J.M. Sanchez-Ruiz, W.A. Eaton, Estimating free-energy barrier heights for an ultrafast folding protein from calorimetric and kinetic data, J. Phys. Chem. B 112 (2008) 5938–5949.
[248] F. Huang, L.M. Ying, A.R. Fersht, Direct observation of barrier-limited folding of BBL by single-molecule fluorescence resonance energy transfer, Proc. Natl. Acad. Sci. USA 106 (2009) 16239–16244.
[249] A.N. Naganathan, U. Doshi, V. Muñoz, Protein folding kinetics: barrier effects in chemical and thermal denaturation experiments, J. Am. Chem. Soc. 129 (2007) 5673–5682.
[250] A. Ansari, C.M. Jones, E.R. Henry, J. Hofrichter, W.A. Eaton, The role of solvent viscosity in the dynamics of protein conformational changes, Science 256 (1992) 1796–1798.

[251] S.J. Hagen, L.L. Qiu, S.A. Pabit, Diffusional limits to the speed of protein folding: fact or friction? J. Phys. Condens. Matter 17 (2005) S1503–S1514.
[252] K.W. Plaxco, D. Baker, Limited internal friction in the rate-limiting step of a two- state protein folding reaction, Proc. Natl. Acad. Sci. USA 95 (1998) 13591–13596.
[253] S.A. Pabit, H. Roder, S.J. Hagen, Internal friction controls the speed of protein folding from a compact configuration, Biochemistry 43 (2004) 12532–12538.
[254] L.L. Qiu, S.J. Hagen, Internal friction in the ultrafast folding of the tryptophan cage, Chem. Phys. 307 (2004) 243–249.
[255] T. Cellmer, E.R. Henry, J. Hofrichter, W.A. Eaton, Measuring internal friction of an ultrafast-folding protein, Proc. Natl. Acad. Sci. USA 105 (2008) 18320–18325.
[256] R. Narayanan, L. Pelakh, S.J. Hagen, Solvent friction changes the folding pathway of the tryptophan zipper TZ2, J. Mol. Biol. 390 (2009) 538–546.
[257] Y.M. Rhee, V.S. Pande, Solvent viscosity dependence of the protein folding dynamics, J. Phys. Chem. B 112 (2008) 6221–6227.
[258] J. Gumbart, L.G. Trabuco, E. Schreiner, E. Villa, K. Schulten, Regulation of the protein-conducting channel by a bound ribosome, Structure 17 (2009) 1453–1464.
[259] F. Noe, C. Schutte, E. Vanden-Eijnden, L. Reich, T.R. Weikl, Constructing the equilibrium ensemble of folding pathways from short off-equilibrium simulations, Proc. Natl. Acad. Sci. USA 106 (2009) 19011–19016.
[260] E. Rosta, N.V. Buchete, G. Hummer, Thermostat artifacts in replica exchange molecular dynamics simulations, J. Chem. Theory Comput. 5 (2009) 1393–1399.
[261] E. Rosta, G. Hummer, Error and efficiency of replica exchange molecular dynamics simulations, J. Chem. Phys. 131 (2009) 165102.
[262] A. Rodriguez-Fortea, A. Laio, F.L. Gervasio, M. Ceccarelli, M. Parrinello, J. Phys. Chem. 109 (2005) 6714.
[263] J. Kim, T. Keyes, J.E. Straub, Replica exchange statistical temperature Monte Carlo, J. Chem. Phys. 130 (2009) 10.
[264] J. Kim, J.E. Straub, T. Keyes, Statistical-temperature Monte Carlo and molecular dynamics algorithms, Phys. Rev. Lett. 97 (2006) 4.
[265] X.W. Wu, B.R. Brooks, Self-guided Langevin dynamics simulation method, Chem. Phys. Lett. 381 (2003) 512–518.
[266] G. Jayachandran, V. Vishal, V.S. Pande, Using massively parallel simulation and Markovian models to study protein folding: examining the dynamics of the villin headpiece, J. Chem. Phys. 124 (2006) 164902.
[267] W. Huisinga, C. Schutte, A.M. Stuart, Extracting macroscopic stochastic dynamics model problems, Commun. Pure Appl. Math. 56 (2003) 234–269.
[268] W.C. Swope, J.W. Pitera, F. Suits, Describing protein folding kinetics by molecular dynamics simulations 1 Theory, J. Phys. Chem. B 108 (2004) 6571–6581.
[269] W.C. Swope, J.W. Pitera, F. Suits, M. Pitman, M. Eleftheriou, B.G. Fitch, R.S. Germain, A. Rayshubski, T.J.C. Ward, Y. Zhestkov, R. Zhou, Describing protein folding kinetics by molecular dynamics simulations 2. Example applications to alanine dipeptide and beta-hairpin peptide, J. Phys. Chem. B 108 (2004) 6582–6594.
[270] D.S. Chekmarev, T. Ishida, R.M. Levy, Long-time conformational transitions of alanine dipeptide in aqueous solution: continuous and discrete-state kinetic models, J. Phys. Chem. B 108 (2004) 19487–19495.
[271] Y. Levy, J. Jortner, R.S. Berry, Eigenvalue spectrum of the master equation for hierarchical dynamics of complex systems, Phys. Chem. Chem. Phys. 4 (2002) 5052–5058.
[272] O.M. Becker, M. Karplus, The topology of multidimensional potential energy surfaces: theory and application to peptide structure and kinetics, J. Chem. Phys. 106 (1997) 1495–1517.
[273] B.L. de Groot, X. Daura, A.E. Mark, H. Grubmüller, Essential dynamics of reversible peptide folding: memory-free conformational dynamics governed by internal hydrogen bonds, J. Mol. Biol. 309 (2001) 299–313.
[274] S. Sriraman, I.G. Kevrekidis, G. Hummer, Coarse master equation from Bayesian analysis of replica molecular dynamics simulations, J. Phys. Chem. B 109 (2005) 6479–6484.
[275] C. Schutte, A. Fischer, W. Huisinga, P. Deuflhard, A direct approach to conformational dynamics based on hybrid Monte Carlo, J. Comp. Phys. 151 (1999) 146–168.
[276] S.V. Krivov, M. Karplus, Hidden complexity of free energy surfaces for peptide (protein) folding, Proc. Natl. Acad. Sci. USA 101 (2004) 14766–14770.
[277] F. Rao, A. Caflisch, The protein folding network, J. Mol. Biol. 342 (2004) 299–306.
[278] E. Rosta, H.L. Woodcock, B.R. Brooks, G. Hummer, Artificial reaction coordinate "tunneling" in free-energy calculations: the catalytic reaction of RNase H, J. Comput. Chem. 30 (2009) 1634–1641.
[279] P.E. McSharry, L.A. Smith, Better nonlinear models from noisy data attractors with maximum likelihood, Phys. Rev. Lett. 83 (1999) 4285–4288.
[280] A. Baba, T. Komatsuzaki, Construction of effective free energy landscape from single-molecule time series, Proc. Natl. Acad. Sci. USA 104 (2007) 19297–19302.
[281] C.B. Li, H. Yang, T. Kornatsuzaki, Multiscale complex network of protein conformational fluctuations in single-molecule time series, Proc. Natl. Acad. Sci. USA 105 (2008) 536–541.
[282] M.C. Prentiss, D.J. Wales, P.G. Wolynes, The energy landscape, folding pathways and the kinetics of a knotted protein, PLoS Comput. Biol. 6 (2010) 12.
[283] D.J. Wales, Energy landscapes: some new horizons, Curr. Opin. Struct. Biol. 20 (2010) 3–10.
[284] A. Rajan, P.L. Freddolino, K. Schulten, Going beyond clustering in MD trajectory analysis: an application to villin headpiece folding, PLoS ONE 5 (2010) 12.
[285] F. Rao, M. Karplus, Protein dynamics investigated by inherent structure analysis, Proc. Natl. Acad. Sci. USA 107 (2010) 9152–9157.
[286] A. Berezhkovskii, A. Szabo, Ensemble of transition states for two-state protein folding from the eigenvectors of rate matrices, J. Chem. Phys. 121 (2004) 9186–9187.
[287] A. Berezhkovskii, G. Hummer, A. Szabo, Reactive flux and folding pathways in network models of coarse-grained protein dynamics, J. Chem. Phys. 130 (2009) 205102.